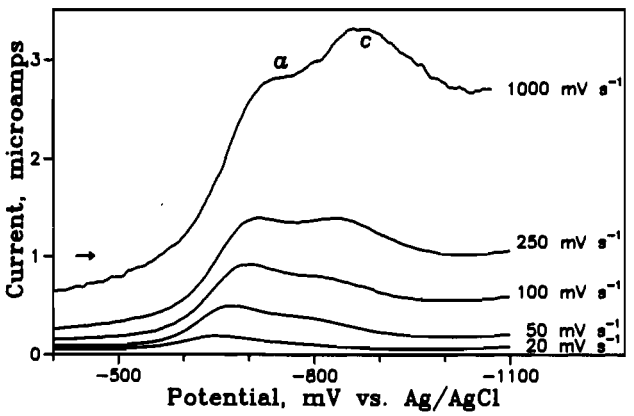

Figure 6. Negative-potential portions of the CV's of $[Et_4N]_2[Ru_4(CO)_{11}(C_2Ph_2)]$ (**3**) under CO (in 0.10 M TBAFB/CH_3CN, Pt working electrode, Ag/AgCl reference) at different scan speeds.

and that the reduction reaction is rapidly followed by the expulsion of a CO ligand. The dianion in the product $[Et_4N]_2[Ru_4(CO)_{11}(C_2Ph_2)]$ (**3**) is a *pseudooctahedral*-Ru_4C_2 cluster that contains two bridging CO groups. Structural comparisons between **3** and **1** revealed little change in the Ru_4C_2 core, indicating electronic stability of the cluster framework toward reduction. In light of the electrochemistry, the *closo*-octahedron description is, perhaps, most appropriate for these alkyne complexes. The isolation of compound **3** and successful digital simulation of the variable scan rate CV's of **1** agree with the mechanism represented in Scheme I.

Acknowledgment. We thank Eric J. Voss for the starting material $Ru_3(CO)_{12}$, Dr. Doris H. Hung for mass spectroscopy, Prof. David Phillips for helpful discussion, and Profs. A. M. Bond and J. W. Lauher for calling our attention to a possible connection between $[Fe_4(CO)_{12}(CC(O)R)]^-$ and the acetylene butterfly compounds. This research was supported by the NSF Synthetic Inorganic and Organometallic Chemistry Program through Grant CHE-8506011.

Supplementary Material Available: For **3**, tables of crystal structure data, positional parameters, thermal parameters, and all bond distances and angles and text describing the program for electrochemical simulation (24 pages); a complete listing of observed and calculated structure factors (27 pages). Ordering information is given on any current masthead page.

Contribution from the Department of Chemistry, University of Minnesota, Minneapolis, Minnesota 55455

Heterometallic Gold-Platinum Phosphine Complexes. 2. X-ray Crystal and Molecular Structures of $[(CO)(PPh_3)Pt(AuPPh_3)_5](Cl)$ and $[(PPh_3)Pt(AuPPh_3)_5(HgNO_3)_2](NO_3)$

Larry N. Ito, Anna Maria P. Felicissimo,† and Louis H. Pignolet*

Received July 13, 1990

In this paper we report the nucleophilic addition reaction of X^- (X = Br, I, CN) and the nucleophilic addition/substitution reaction of tertiary phosphites L = $P(OMe)_3$ or $P(OCH_2)_3CCH_3$ to the 16-electron cluster $[(PPh_3)Pt(AuPPh_3)_6]^{2+}$ (**7**), giving the new 18-electron complexes $[(X)(PPh_3)Pt(AuPPh_3)_6]^+$ (**9**) and $[(L)_2Pt(AuPPh_3)_6]^{2+}$ (**10**), respectively. An unusual oxidative-addition reaction of $Hg_2(NO_3)_2$ to **7** with elimination of $AuPPh_3^+$ giving the 18-electron product $[(PPh_3)Pt(AuPPh_3)_5(HgNO_3)_2]^+$ (**11**) has also been carried out. These reactions are shown in Scheme II. Some nucleophilic and electrophilic addition reactions that illustrate the above reactivity priniciple and that give six new $PtAu_x$ clusters with x = 3 and 4 have also been carried out as shown in Scheme I. These complexes have been characterized by IR, FABMS, and ^{31}P and ^{13}C NMR spectroscopy. X-ray crystal structure determinations have been carried out on the 18-electron clusters $[(CO)(PPh_3)Pt(AuPPh_3)_5]^+$ (**8**) and $[(PPh_3)Pt(AuPPh_3)_5(HgNO_3)_2]^+$ (**11**), and their metal core geometries, which are spheroidal fragments of centered icosahedrons, are in agreement with predictions based on electron counting. The crystal data for these complexes are as follows. **8**(Cl)·$(CH_3CH_2)_2O$: monoclinic, $C2/c$, a = 35.91 (1) Å, b = 29.637 (7) Å, c = 26.025 (7) Å, β = 132.62 (2)°, V = 20,383 Å^3, Z = 8; residuals R = 0.075 and R_w = 0.085 for 4815 observed reflections and 263 variables; Mo Kα radiation. **11**(NO_3)·$3CH_2Cl_2$: triclinic, $P\bar{1}$, a = 14.18 (1) Å, b = 17.92 (1) Å, c = 22.91 (2) Å, α = 89.68 (7)°, β = 84.80 (7)°, γ = 69.18 (7)°, V = 5415 Å^3, Z = 2; residuals R = 0.062 and R_w = 0.073 for 7822 observed reflections and 411 variables; Mo Kα radiation.

Introduction

A number of platinum-centered heterobimetallic cluster complexes of the general formulation $[(L)_yPt(AuPPh_3)_x]^{n+}$, where L = ligand (for example PPh_3, CO, RC≡C, H, NO_3) and/or metal (for example Ag or Hg) and x = 2, 6, 7, and 8, have recently been reported. Some of the well-characterized examples include $[(PPh_3)_2(NO_3)Pt(AuPPh_3)_2]^+$,[1] $[(C{\equiv}C{-}t\text{-}Bu)(PPh_3)Pt(AuPPh_3)_6]^+$,[2] $[(PPh_3)Pt(AuPPh_3)_6]^{2+}$,[3] $[(CO)(PPh_3)Pt(AuPPh_3)_6]^{2+}$,[3] $[(PPh_3)(H)Pt(AuPPh_3)_7]^{2+}$,[4,5] $[Pt(AuPPh_3)_8]^{2+}$,[6] $[(CO)Pt(AuPPh_3)_8]^{2+}$,[6] $[(AgNO_3)Pt(AuPPh_3)_8]^{2+}$,[7] $[(AgNO_3)(CO)Pt(AuPPh_3)_8]^{2+}$,[7] and $[(Hg)_2Pt(AuPPh_3)_8]^{4+}$.[8,9] These complexes form a series of $PtAu_x$ clusters that have shown a variety of novel structures and interesting reactivity.[1-10] In this paper we report the synthesis and characterization of six new $PtAu_x$ clusters with x = 3 and 4 (complexes **1-6** in Scheme I) and thus add the important missing members of the x = 2-8 series. Such a complete series of cluster complexes should prove important in studies of metal-particle physics, chemical bonding, reactivity,

† Institute of Chemistry, University of São Paulo, São Paulo, Brazil.

(1) Boyle, P. D.; Johnson, B. J.; Alexander, B. D.; Casalnuovo, J. A.; Gannon, P. R.; Johnson, S. M.; Larka, E. A.; Mueting, A. M.; Pignolet, L. H. *Inorg. Chem.* **1987**, *26*, 1346.
(2) Smith, E. W.; Welch, A. J.; Treurnicht, I.; Puddephatt, R. J. *Inorg. Chem.* **1986**, *25*, 4616.
(3) Ito, L. N.; Sweet, J. D.; Mueting, A. M.; Pignolet, L. H.; Schoondergang, M. F. J.; Steggerda, J. J. *Inorg. Chem.* **1989**, *28*, 3696.
(4) Kanters, R. P. F.; Bour, J. J.; Schlebos, P. P. J.; Bosman, W. P.; Behm, H.; Steggerda, J. J.; Ito, L. N.; Pignolet, L. H. *Inorg. Chem.* **1989**, *28*, 2591.
(5) Bour, J. J.; Kanters, R. P. F.; Schlebos, P. P. J.; Steggerda, J. J. *Recl. Trav. Chim. Pays-Bas* **1988**, *107*, 211.
(6) Kanters, R. P. F.; Schlebos, P. P. J.; Bour, J. J.; Bosman, W. P.; Behm, H. J.; Steggerda, J. J. *Inorg. Chem.* **1988**, *27*, 4034. Bour, J. J.; Kanters, R. P. F.; Schlebos, P. P. J.; Bosman, W. P.; Behm, H.; Beurskens, P. T.; Steggerda, J. J. *Recl.: J. R. Neth. Chem. Soc.* **1987**, *106*, 157. Bour, J. J.; Kanters, R. P. F.; Schlebos, P. P. J.; Steggerda, J. J. *Recl.: J. R. Neth. Chem. Soc.* **1988**, *107*, 211.
(7) Kanters, R. P. F.; Schlebos, P. P. J.; Bour, J. J.; Bosman, W. P.; Smits, J. M. M.; Beurskens, P. T.; Steggerda, J. J. *Inorg. Chem.* **1990**, *29*, 324.

0020-1669/91/1330-0387$02.50/0

Scheme I

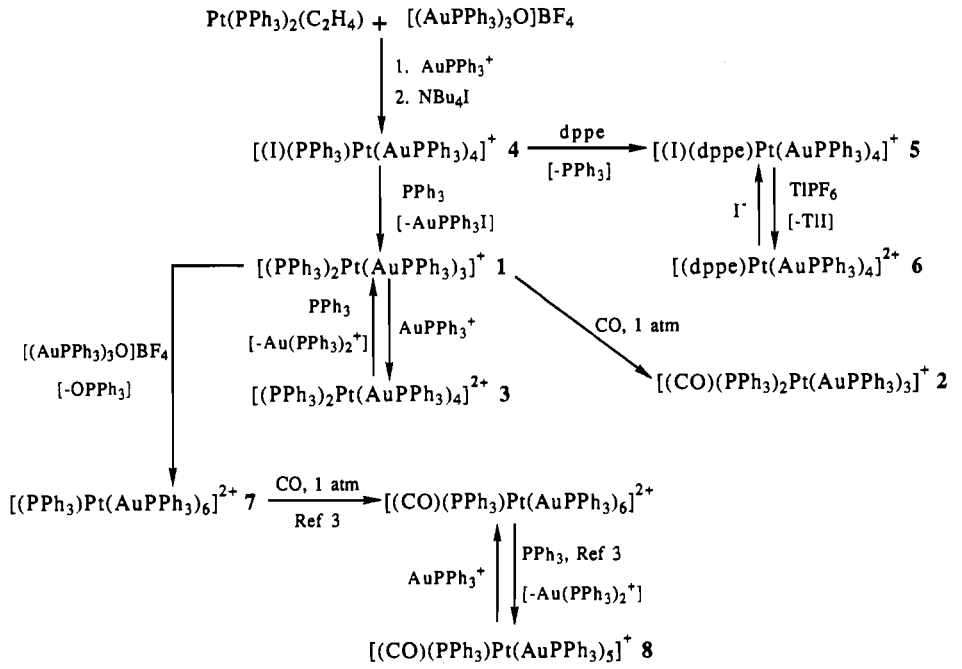

and bimetallic catalyst models.[3,7,10-12]

The above cluster complexes are all platinum centered and can be classified as having 16 or 18 Pt valence electrons. In electron counting for these complexes, the central Pt contributes 10 electrons, each $AuPPh_3$ unit contributes 1 electron, PR_3 and CO contribute 2 electrons, halides, $RC{\equiv}C$, NO_3, and H contribute 1 electron, $AgNO_3$ contributes 0 electrons, $HgNO_3$ contributes 1 electron, and Hg contributes 2 electrons. This electron count has been shown to be useful in predicting reactivity[3,6,7] and structure.[11,12] The 16-electron clusters undergo nucleophilic addition reactions to achieve the stable 18-electron configuration as well as electrophilic additions, while the 18-electron clusters undergo only electrophilic additions. Examples of nucleophilic addition of CO and electrophilic addition of $AgNO_3$ to a 16-electron cluster are[6,7]

$$[Pt(AuPPh_3)_8]^{2+} + CO \rightarrow [(CO)Pt(AuPPh_3)_8]^{2+}$$

$$[Pt(AuPPh_3)_8]^{2+} + AgNO_3 \rightarrow [(AgNO_3)Pt(AuPPh_3)_8]^{2+}$$

An example of an electrophilic addition of $AgNO_3$ to an 18-electron cluster is[7]

$$[(CO)Pt(AuPPh_3)_8]^{2+} + AgNO_3 \rightarrow [(AgNO_3)(CO)Pt(AuPPh_3)_8]^{2+}$$

In this paper we report the nucleophilic addition reaction of X^- (X = Br, I, CN) and the nucleophilic addition/substitution reaction of tertiary phosphites L = $P(OMe)_3$ or $P(OCH_2)_3CCH_3$ to the 16-electron cluster $[(PPh_3)Pt(AuPPh_3)_6]^{2+}$ (**7**), giving the new 18-electron complexes $[(X)(PPh_3)Pt(AuPPh_3)_6]^+$ (**9**) and $[(L)_2Pt(AuPPh_3)_6]^{2+}$ (**10**), respectively. An unusual oxidative-addition reaction of $Hg_2(NO_3)_2$ with elimination of $AuPPh_3^+$ giving the 18-electron product $[(PPh_3)Pt(AuPPh_3)_5(HgNO_3)_2]^+$ (**11**) has also been carried out. These reactions and others are shown in Scheme II. Some nucleophilic and electrophilic addition reactions that illustrate the above reactivity principle and that

Scheme II

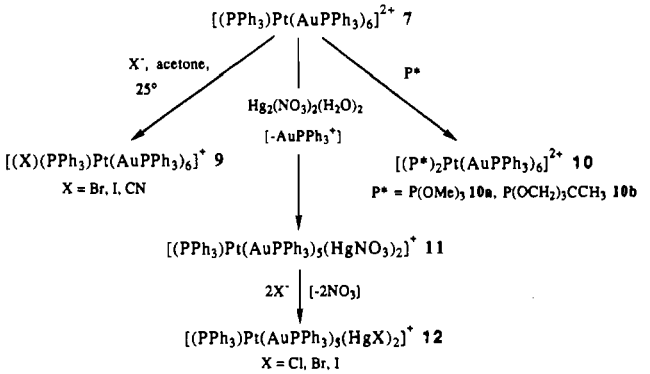

give the new $PtAu_x$ clusters **1**–**6** with $x = 3$ and 4 have also been carried out as outlined in Scheme I. X-ray crystal structures are reported on clusters **8** and **11**, and their metal core geometries are in agreement with predictions based on electron counting.[3,6,7,11,12]

Experimental Section

Physical Measurements and Reagents. ^{31}P NMR spectra were recorded at 121.5 MHz with use of a Nicolet NT-300 or a Varian VXR-300 MHz spectrometer. ^1H NMR spectra were recorded at 300 MHz and ^{13}C spectra were recorded at 75.5 MHz with use of a varian VXR 300-MHz spectrometer. Both were run with proton decoupling, and ^{31}P NMR spectra are reported in ppm relative to internal standard trimethyl phosphate (TMP), with positive shifts downfield. ^{13}C NMR spectra are reported in ppm relative to external standard tetramethylsilane (TMS), with positive shifts downfield. Infrared spectra were recorded on a Perkin-Elmer 1710 FT-IR spectrometer. Conductivity measurements were made with use of a Yellow Springs Model 31 conductivity bridge. Compound concentrations used in the conductivity experiments were 3×10^{-4} M in CH_3CN. FABMS experiments were carried out with use of a VG Analytical, Ltd., 7070E-HF high-resolution double-focusing mass spectrometer equipped with a VG 11/250 data system.[1,10] Microanalyses were carried out by Analytische Laboratorien, Engelskirchen, West Germany. Solvents were dried and distilled prior to use. $[(PPh_3)Pt(AuPPh_3)_6](NO_3)_2$ (**7**$(NO_3)_2$),[3] $[(CO)(PPh_3)Pt(AuPPh_3)_6](NO_3)_2$,[3] $[(CO)(PPh_3)Pt(AuPPh_3)_5](Cl)$ (**8**(Cl)),[3] $Pt(C_2H_4)(PPh_3)_2$,[13] $[(AuPPh_3)_3O]BF_4$,[14] $P(OCH_2)_3CCH_3$,[15] and $Au(PPh_3)NO_3$[16] were pre-

(8) Bour, J. J.; Berg, W. v. d.; Schlebos, P. P.; Kanters, R. P. F.; Schoondergang, M. F. J.; Bosman, W. P.; Smits, J. M. M.; Beurskens, P. T.; Steggerda, J. J.; van der Sluis, P. *Inorg. Chem.* **1990**, *29*, 2971.
(9) Kanters, R. P. F.; Bour, J. J.; Schlebos, P. P. J.; Steggerda, J. J. *J. Chem. Soc., Chem. Commun.* **1988**, 1634.
(10) Mueting, A. M.; Bos, W.; Alexander, B. D.; Boyle, P. D.; Casalnuovo, J. A.; Balaban, S.; Ito, L. N.; Johnson, S. M.; Pignolet, L. H. In *Recent Advances in Di- and Polynuclear Chemistry*; Braunstein, P., Ed.; *New J. Chem.* **1988**, *12*, 505 and references cited therein.
(11) Stone, A. J. *Inorg. Chem.* **1981**, *20*, 563.
(12) Mingos, D. M. P.; Johnston, R. L. *Struct. Bonding* **1987**, *68*, 29.
(13) Cook, C. D.; Jauhal, G. S. *J. Am. Chem. Soc.* **1968**, *90*, 1464.
(14) Bruce, M. I.; Nicholson, B. K.; Shawkataly, O. B. *Inorg. Synth.* **1989**, *26*, 324.

pared as described in the literature. All manipulations were carried out under a purified N_2 atmosphere with use of standard Schlenk techniques unless otherwise noted.

Preparation of Complexes. $[(PPh_3)_2Pt(AuPPh_3)_3](PF_6)$ (1(PF_6)). Method A. A 100-mL Schlenk flask was charged with $[(I)(PPh_3)Pt(AuPPh_3)_4]BF_4$ (4(BF_4)) (0.306 g, 0.122 mmol), PPh_3 (0.032 g, 0.122 mmol), and a magnetic stir bar. The reactants were dissolved in acetone (6 mL) and stirred at 25 °C. After 1 min a white solid precipitated. CH_3OH (30 mL) was then added to the reactant mixture. After 10 min of stirring the mixture was filtered through a fritted glass filter. The filtrate was evaporated to dryness under reduced pressure. The dark orange solid residue was dissolved in a minimal amount of CH_2Cl_2 and the solution was added to a stirring solution containing NH_4PF_6 (0.20 g, 1.2 mmol) in MeOH (4 mL). The orange solid that precipitated was isolated on a fritted glass filter, washed with MeOH (5 mL) and Et_2O (10 mL), and dried under vacuum. Red crystals were obtained by slow solvent diffusion of Et_2O into a CH_2Cl_2 solution containing $[(PPh_3)_2Pt(AuPPh_3)_3](PF_6)$. The yield was 240 mg (90.2%) after recrystallization. Compound 1(PF_6) is soluble in CH_2Cl_2, chloroform, and acetone and insoluble in saturated hydrocarbons and Et_2O. ^{31}P NMR (CD_2Cl_2, 20 °C): δ 60.2 (q with ^{195}Pt satellites, $^3J_{P-P}$ = 44 Hz, $J_{^{195}Pt-P}$ = 3673 Hz, int = 2), 47.3 (t with ^{195}Pt satellites, $^3J_{P-P}$ = 44 Hz, $^2J_{^{195}Pt-P}$ = 505 Hz, int = 3). IR (KBr): $\nu(PF_6)$ 839 cm^{-1}. The equivalent conductance (115.0 cm^2 mhos mol^{-1}) is indicative of a 1:1 electrolyte in CH_3CN solution. FABMS (*m*-nitrobenzyl alcohol matrix): *m/z* 2097 ($[(PPh_3)_2Pt(AuPPh_3)_3]^+ = M^+$), 1835 ($(M - PPh_3)^+$). **Method B.** A 100-mL Schlenk flask was charged with $[Pt(PPh_3)_2(C_2H_4)]$ (0.040 g, 0.0535 mmol), $[(AuPPh_3)_3O]BF_4$ (0.080 g, 0.0541 mmol), and a magnetic stir bar. The reactants were dissolved in acetone (10 mL) at 0 °C. After 10 min of stirring, Et_2O was added to precipitate an orange solid. The orange precipitate was isolated on a fritted glass filter, washed with Et_2O (10 mL), and dried under vacuum. The solid analyzed by ^{31}P NMR spectroscopy contained **1** and $PPh_3Pt(AuPPh_3)_6^{2+}$ (**7**).[3] Efforts to separate these two compounds were unsuccessful.

$[(CO)(PPh_3)_2Pt(AuPPh_3)_3](PF_6)$ (2(PF_6)) was prepared dissolving **1** (50 mg, 0.022 mmol) in CH_2Cl_2 (10 mL) and placing the solution under 1 atm of CO. The color of the solution changed from golden yellow to pale yellow immediately. The volume of the solution was reduced to 2 mL and transferred to a magnetically stirred flask containing Et_2O (60 mL). The yellow precipitate was collected on a fritted glass filter, washed with Et_2O (40 mL), and dried under vacuum. Yield: 48 mg (95%). 2(PF_6) is soluble in CH_2Cl_2, chloroform, and acetone and insoluble in saturated hydrocarbons and Et_2O. The isotopically labeled analogue $[(^{13}CO)(PPh_3)_2Pt(AuPPh_3)_3](PF_6)$ was prepared by the same procedure using ^{13}CO. ^{31}P NMR (CD_2Cl_2, 20 °C): δ 45.6 (t with ^{195}Pt satellites, $^3J_{P-P}$ = 38.5 Hz, $^2J_{^{195}Pt-P}$ = 480 Hz, int = 3), 32.9 (q with ^{195}Pt satellites, $^3J_{P-P}$ = 38.5 Hz, $J_{^{195}Pt-P}$ = 2633 Hz, int = 2). ^{13}C NMR (CD_2Cl_2, 20 °C): δ 198.3 (q with ^{195}Pt satellites, $J_{^{13}C-Pt}$ = 1352; $^3J_{^{13}C-P}$ = 15.6 Hz). IR (KBr): ν(CO) 1974, $\nu(^{13}CO)$ 1924 [$\nu(CO)/\nu(^{13}CO)$ = 1.026], $\nu(PF_6)$ 840 cm^{-1}. The equivalent conductance (116.2 cm^2 mhos mol^{-1}) is indicative of a 1:1 electrolyte in CH_3CN solution.

$[(PPh_3)_2Pt(AuPPh_3)_4](PF_6)_2$ (3(PF_6)$_2$). A 100-mL Schlenk flask was charged with 1(PF_6) (0.099 g, 0.0441 mmol), PPh_3AuNO_3 (0.046 g, 0.088 mmol), and a magnetic stir bar. The reactants were dissolved in acetone (6 mL) and stirred at 25 °C. After 10 min the solvent was removed under reduced pressure. The brown solid was dissolved in CH_2Cl_2 (1 mL), and the mixture was added to a stirred solution of NH_4PF_6 (87 mg, 0.533 mmol) in MeOH (3 mL). The dark red precipitate was isolated on a fritted glass filter, washed with MeOH (10 mL) and Et_2O (10 mL), and dried under vacuum. Dark red crystals were obtained by slow solvent diffusion of Et_2O (15 mL) into a CH_2Cl_2 solution (2 mL) containing $[(PPh_3)_2Pt(AuPPh_3)_4](PF_6)_2$. The yield was 90 mg (71%) after recrystallization. 3(PF_6)$_2$ is soluble in CH_2Cl_2, chloroform, and acetone and insoluble in saturated hydrocarbons and Et_2O. ^{31}P NMR (CD_2Cl_2, 20 °C): δ 53.9 (pentent with ^{195}Pt satellites, $^3J_{P-P}$ = 47.6 Hz, $J_{^{195}Pt-P}$ = 3234 Hz, int = 1), 44.0 (t with ^{195}Pt satellites, $^3J_{P-P}$ = 47.6 Hz, $^2J_{^{195}Pt-P}$ = 377 Hz, int = 2). The ^{31}P NMR spectrum broadened as the temperature was lowered and at −100 °C began to freeze out, giving broad resonances with ^{195}Pt–P coupling: δ 48.9 ($J_{^{195}Pt-P}$ = 3271 Hz, int = 2), 47.0 ($^2J_{^{195}Pt-P}$ = 504 Hz, int = 2), 42.2 ($^2J_{^{195}Pt-P}$ = 226 Hz, int = 1), 41.9 ($^2J_{^{195}Pt-P}$ = 226 Hz, int = 1) IR (KBr): $\nu(PF_6)$ 839 cm^{-1}. The equivalent conductance (172.0 cm^2 mhos mol^{-1}) is indicative of a 2:1 electrolyte in CH_3CN solution. FABMS (*m*-nitrobenzyl alcohol matrix): *m/z* 2701 ($[(PPh_3)_2Pt(AuPPh_3)_4(PF_6)]^+ = M^+$), 2439 ($(M - PPh_3)^+$), 2294 ($(M - PPh_3 - PF_6)^+$), 2096 ($(M - AuPPh_3 - PF_6)^+$), 2032 ($(M - 2PPh_3 - PF_6)^+$). Anal. Calcd for $Au_4PtP_8C_{108}H_{90}F_{12}\cdot CH_2Cl_2$: C, 44.66; H, 3.16; P, 8.45. Found: C, 44.14; H, 2.99; P, 8.61.

$[(I)(PPh_3)Pt(AuPPh_3)_4](BF_4)$ (4(BF_4)). A 100-mL Schlenk flask was charged with $[(AuPPh_3)_3O]BF_4$ (0.221 g, 0.149 mmol), $Pt(PPh_3)_2(C_2H_4)$ (0.112 g, 0.150 mmol), and a magnetic stir bar. CH_2Cl_2 (8 mL) was added to the reaction vessel at 0 °C and the orange solution stirred for 5 min. PPh_3AuNO_3 (0.078 g, 0.150 mmol) was added as a solid, and the color of the solution changed from orange to brown immediately. NBu_4I (0.055 g, 0.152 mmol) was then added to the reaction flask, and the color of the solution changed from brown to orange immediately. After the solution was stirred for 5 min, the solvent was removed under vacuum. The solid was dissolved in acetone (8 mL) and the solution filtered through diatomaceous earth into a Schlenk flask. MeOH (10 mL) was added to the solution and the acetone removed under vacuum to precipitate a bright orange solid. The precipitate was isolated on a fritted glass filter, washed with MeOH (10 mL) and Et_2O (10 mL) and dried under vacuum. Yield: 265 mg (71%). $[(I)(PPh_3)Pt(AuPPh_3)_4](BF_4)$ is soluble in CH_2Cl_2, chloroform, and acetone and insoluble in saturated hydrocarbons and Et_2O. ^{31}P NMR (CD_2Cl_2, 20 °C): δ 57.6 (pentet with ^{195}Pt satellites, $^3J_{P-P}$ = 44.0 Hz, $J_{^{195}Pt-P}$ = 4131 Hz, int = 1), 43.4 (d with ^{195}Pt satellites, $^3J_{P-P}$ = 44.0 Hz, $^2J_{^{195}Pt-P}$ = 498 Hz, int = 4). IR (KBr): $\nu(BF_4)$ 1085 cm^{-1}. The equivalent conductance (98.1 cm^2 mho mol^{-1}) is indicative of a 1:1 electrolyte in CH_3CN solution. FABMS (*m*-nitrobenzyl alcohol matrix): *m/z* 2421 ($[(I)(PPh_3)Pt(AuPPh_3)_4]^+ = M^+$), 218 ($(M - PPh_3)^+$), 1962 ($(M - Au - PPh_3)^+$). The PF_6 salt of **4**, 4(PF_6), was made by the following method. 4(BF_4) (100 mg, 0.0398 mmol) was dissolved in CH_2Cl_2 (1 mL), and the mixture was added to a stirred solution containing NH_4PF_6 (65 mg, 0.398 mmol) in MeOH (2 mL). The orange precipitate was isolated on a fritted glass filter, washed with MeOH and Et_2O, and dried under vacuum. Orange crystals were obtained by slow solvent diffusion of Et_2O (15 mL) into a CH_2Cl_2 solution (3 mL) that contained $[(I)(PPh_3)Pt(AuPPh_3)_4](PF_6)$. The yield was 101 mg (94%) after recrystallization. 4(PF_6) is soluble in CH_2Cl_2, chloroform, and acetone and insoluble in alcohols, saturated hydrocarbons, and Et_2O. The ^{31}P NMR spectrum (CD_2Cl_2, 20 °C) was identical with that of the BF_4 salt. IR (KBr): $\nu(PF_6)$ 839 cm^{-1}. The equivalent conductance (85.4 cm^2 mhos mol^{-1}) is indicative of a 1:1 electrolyte in CH_3CN solution. Anal. Calcd for $Au_4PtP_6C_{90}H_{75}F_6I$: C, 42.12; H, 2.95; P, 7.24. Found: C, 41.99; H, 2.84; P, 7.88.

$[(I)(dppe)Pt(AuPPh_3)_4](PF_6)$ (5(PF_6)). A 20-mL Schlenk tube was charged with 4(PF_6) (0.075 g, 0.0292 mmol) and dppe (1,2-bis(diphenylphosphino)ethane) (0.012 g, 0.0301 mmol). The reactants were dissolved in CH_2Cl_2 (2 mL). After 5 min Et_2O (7 mL) was added to the reaction vessel and the flask allowed to stand undisturbed. After 8 h dark yellow crystals precipitated. The crystals were isolated on a fritted glass filter, washed with Et_2O (10 mL), and dried under vacuum. Yield: 67 mg (85%). 5(PF_6) is soluble in CH_2Cl_2, chloroform, and acetone and insoluble in saturated hydrocarbons and Et_2O. ^{31}P NMR (1,1,2-trichloroethane, 75 °C): δ 76.6 (pentet with ^{195}Pt satellites, $^3J_{P-P}$ = 45.7 Hz, $J_{^{195}Pt-P}$ = 3236 Hz, int = 1), 50.7 (t with ^{195}Pt satellites, $^3J_{P-P}$ = 45.7 Hz, $^2J_{^{195}Pt-P}$ = 324 Hz, int = 2). IR (KBr): $\nu(PF_6)$ 839 cm^{-1}. The conductance (94.6 cm^2 mhos mol^{-1}) indicative of a 1:1 electrolyte in CH_3CN solution. Anal. Calcd for $Au_4PtP_4C_{98}H_{38}F_6I\cdot CH_2Cl_2$: C, 42.66; H, 3.11; P, 7.78. Found: C, 42.64; H, 3.00; P, 8.02.

$[(dppe)Pt(AuPPh_3)_4](PF_6)_2$ (6(PF_6)$_2$). A 20-mL Schlenk tube was charged with 5(PF_6) (0.065 g, 0.0241 mmol) and a magnetic stir bar. CH_2Cl_2 (5 mL) was added to the reaction vessel. After stirring for 10 min a solution of $TlPF_6$ (10 mg, 0.0286 mmol) dissolved in CH_3CN (1 mL) was added to the stirred CH_2Cl_2 solution containing $[(I)(dppe)Pt(AuPPh_3)_4](PF_6)$. A light yellow solid (TlI) precipitated immediately. The mixture was filtered through a bed of diatomaceous earth on a fritted glass filter. Et_2O was added in small portions to the filtrate with mixing until the beginning of crystallization. After 8 h the orange crystals were isolated on a fritted glass filter, washed with Et_2O (10 mL), and dried under vacuum. Yield: 59 mg (90%). 6(PF_6)$_2$ is soluble in CH_2Cl_2, chloroform, and acetone and insoluble in saturated hydrocarbons and Et_2O. ^{31}P NMR (CD_2Cl_2, 20 °C): δ 82.2 (pentet with ^{195}Pt satellites, $^3J_{P-P}$ = 47.6 Hz, $J_{^{195}Pt-P}$ = 3098 Hz, int = 1), 50.7 (t with ^{195}Pt satellites, $^3J_{P-P}$ = 47.6 Hz, $^2J_{^{195}Pt-P}$ = 363 Hz, int = 2). ^1H NMR (CD_2Cl_2, 20 °C): δ 7.8–6.8 (m, phenyl Hs, int = 20), 2.41 (m, CH_2CH_2, int = 1). IR (KBr): $\nu(PF_6)$ 839 cm^{-1}. The equivalent conductance (178.2 cm^2 mhos mol^{-1}) is indicative of a 2:1 electrolyte in CH_3CN solution. FABMS (*m*-nitrobenzyl alcohol matrix): *m/z* 2575 ($[(dppe)Pt(AuPPh_3)_4(PF_6)]^+ = M^+$), 2430 ($(M - PF_6)^+$), 2168 ($(M - PPh_3 - PF_6)^+$).

$[(X)(PPh_3)Pt(AuPPh_3)_6](NO_3)$ (9(NO_3), X = 1) was prepared by placing 7(NO_3)$_2$ (50 mg, 0.015 mmol) and NBu_4I (5.2 mg, 0.015 mmol) in a Schlenk tube and dissolving the reactants in acetone (2 mL). The color of the solution changed from brown to dark purple immediately, and dark purple crystals began to precipitate. The crystals were isolated on a fritted glass filter, washed with acetone (10 mL) and Et_2O (10 mL),

(15) Verkade, J. G.; Piper, T. S. *Inorg. Chem.* **1963**, *2*, 944.
(16) Malatesta, L.; Naldini, L.; Simonetta, G.; Cariati, F. *Coord. Chem. Rev.* **1966**, *1*, 255.

and dried under vacuum. Yield: 48 mg (96%). **9**(NO_3), X = I, is soluble in CH_2Cl_2, chloroform, and acetone and insoluble in alcohols, saturated hydrocarbons, and Et_2O. It is air, light, and moisture stable in the solid state. ^{31}P NMR (CD_2Cl_2, 20 °C): δ 56.8 (sept with ^{195}Pt satellites, $^3J_{P-P}$ = 36.6 Hz, $J_{^{195}Pt-P}$ = 3379 Hz, int = 1), 45.4 (d with ^{195}Pt satellites, $^3J_{P-P}$ = 36.6 Hz, $^2J_{^{195}Pt-P}$ = 493 Hz, int = 6). IR (KBr): $\nu(NO_3)$ 1341 cm^{-1}. **9**(NO_3), X = Br, was prepared in a fashion similar to that for **9**(NO_3), X = I, by replacing NBu_4Br for NBu_4I. **9**(NO_3), X = Br, is soluble in CH_2Cl_2, chloroform, and acetone and insoluble in alcohols, saturated hydrocarbons, and Et_2O. ^{31}P NMR (CD_2Cl_2, 20 °C): δ 60.8 (sept with ^{195}Pt satellites, $^3J_{P-P}$ = 31.7 Hz, $J_{^{195}Pt-P}$ = 3667 Hz, int = 1), 48.3 (d with ^{195}Pt satellites, $^3J_{P-P}$ = 31.7 Hz, $^2J_{^{195}Pt-P}$ = 439 Hz, int = 6). IR (KBr): $\nu(NO_3)$ 1341 cm^{-1}. **9**(NO_3), X = CN, was prepared in a fashion similar to that for **9**(NO_3), X = I, by replacing KCN for NBu_4I and using MeOH as the solvent. **9**(NO_3), X = CN, is soluble in CH_2Cl_2, chloroform, and acetone and insoluble in saturated hydrocarbons and Et_2O. It is air, light, and moisture stable in the solid state. ^{31}P NMR (CD_2Cl_2, 20 °C): δ 59.2 (sept with ^{195}Pt satellites, $^3J_{P-P}$ = 41.5 Hz, $J_{^{195}Pt-P}$ = 2222 Hz, int = 1), 44.6 (d with ^{195}Pt satellites, $^3J_{P-P}$ = 41.5 Hz, $^2J_{^{195}Pt-P}$ = 415 Hz, int = 6). IR (KBr): ν(CN) 2073, $\nu(NO_3)$ 1341 cm^{-1}. The equivalent conductance (96.2 cm^2 mhos mol^{-1}) is indicative of a 1:1 electrolyte in CH_3CN solution.

[(P(OCH$_3$)$_3$)$_2$Pt(AuPPh$_3$)$_6$](NO$_3$)$_2$ (10a(NO$_3$)$_2$) was prepared by dissolving **7**$(NO_3)_2$ (50 mg, 0.015 mmol) in CH_2Cl_2 (2 mL) in a Schlenk tube and adding $P(OCH_3)_3$ (7 μL, 0.059 mmol) to the reaction vessel. The color of the solution changed immediately from brown to red. Et_2O was added in small portions with mixing until crystallization began. The red crystals were isolated on a fritted glass filter, washed with Et_2O (10 mL), and dried under vacuum. Yield: 45 mg (89.1%). **10a**$(NO_3)_2$ is soluble in alcohols, CH_2Cl_2, chloroform, and acetone and insoluble in saturated hydrocarbons and Et_2O. ^{31}P NMR (CD_2Cl_2, 20 °C): δ 157.0 (sept with ^{195}Pt satellites, $^3J_{P-P}$ = 55.1 Hz, $J_{^{195}Pt-P}$ = 4205 Hz, int = 1), 49.0 (t with ^{195}Pt satellites, $^3J_{P-P}$ = 55.1 Hz, $^2J_{^{195}Pt-P}$ = 362 Hz, int = 3). ^1H NMR (CD_2Cl_2, 20 °C): δ 7.4–6.7 (m, phenyl H's, int = 5), 3.33 (m, OCH_3, int = 1). IR (KBr): $\nu(NO_3)$ 1341 cm^{-1}. The equivalent conductance (188.8 cm^2 mhos mol^{-1}) is indicative of a 2:1 electrolyte in CH_3CN solution.

[(P(OCH$_2$)$_3$CCH$_3$)$_2$Pt(AuPPh$_3$)$_6$](NO$_3$)$_2$ (10b(NO$_3$)$_2$ was prepared in a fashion similar to that for **10a**$(NO_3)_2$ by substituting $P(OCH_2)_3CCH_3$ for $P(OCH_3)_3$. **10b**$(NO_3)_2$ is soluble in alcohols, CH_2Cl_3, chloroform, and acetone and insoluble in saturated hydrocarbons and Et_2O. ^{31}P NMR (CD_2Cl_2, 20 °C): δ 171.1 (sept with ^{195}Pt satellites, $^3J_{P-P}$ = 57.5 Hz, $J_{^{195}Pt-P}$ = 4107 Hz, int = 1), 49.2 (t with ^{195}Pt satellites, $^3J_{P-P}$ = 57.5 Hz, $^2J_{^{195}Pt-P}$ = 366 Hz, int = 3). ^1H NMR (CD_2Cl_2, 20 °C): δ 7.8–6.8 (m, phenyl H's, int = 15), 4.32 (s (br), OCH_2, int = 2), 1.31 (s (br), CCH_3, int = 1). IR (KBr): $\nu(NO_3)$ 1341 cm^{-1}. The equivalent conductance (214.2 cm^2 mhos mol^{-1}) is indicative of a 2:1 electrolyte in CH_3CN solution.

[(PPh$_3$)Pt(AuPPh$_3$)$_5$(HgNO$_3$)$_2$](NO$_3$) (11(NO$_3$)). A 100-mL Schlenk flask was charged with **7**$(NO_3)_2$ (0.400 g, 0.120 mmol), $Hg_2(NO_3)_2(H_2O)_2$ (0.070 g, 0.124 mmol), and a magnetic stir bar. The reactants were dissolved in MeOH (30 mL) at 0 °C. After the solution was stirred for 15 min at 0 °C, the solvent was removed under reduced pressure. The orange solid was dissolved in CH_2Cl_2 (10 mL), and the mixture was filtered through a bed of diatomaceous earth on a fritted glass filter. The filtrate was evaporated to dryness under reduced pressure. The orange solid was dissolved in MeOH (10 mL), and the solution was transferred to a Schlenk tube. Et_2O (30 mL) was added to the MeOH solution containing $[(PPh_3)Pt(AuPPh_3)_5(HgNO_3)_2](NO_3)$. After 8 h, dark orange crystals precipitated. The crystals were isolated on a fritted glass filter, washed with Et_2O, and dried under vacuum. The yield was 310 mg (77%) after recrystallization. **11**(NO_3) is soluble in alcohols, CH_2Cl_2, chloroform, and acetone and insoluble in saturated hydrocarbons and Et_2O. ^{31}P NMR (CD_2Cl_2, 20 °C): δ 54.9 (sext with ^{195}Pt satellites, $^3J_{P-P}$ = 39.7 Hz, $J_{^{195}Pt-P}$ = 3258 Hz, $^2J_{^{199}Hg-P}$ unobserved, int = 1), 53.1 (d with ^{195}Pt satellites, $^3J_{P-P}$ = 39.7 Hz, $^2J_{^{199}Hg-P}$ = 604 Hz, $^2J_{^{195}Pt-P}$ = 390 Hz, int = 5). IR (KBr): $\nu(NO_3)$ 1341 (unbound), 1255 cm^{-1} (bound). The equivalent conductance (155.5 cm^2 mhos mol^{-1}) is indicative of a 1:1 electrolyte in CH_3CN solution. FABMS (*m*-nitrobenzyl alcohol matrix): *m/z* 3279 ($[(PPh_3)Pt(AuPPh_3)_5(HgNO_3)_2]$ = M^+), 2754 ((M = PPh_3 - $HgNO_3)^+$), 2553 ((M - PPh_3 - 2Hg - $NO_3)^+$), 2356 ((M - $AuPPh_3$ - 2Hg - $NO_3)^+$), 2294 ((M - $AuPPh_3$ - $2HgNO_3)^+$).

[(PPh$_3$)Pt(AuPPh$_3$)$_5$(HgX)$_2$](NO$_3$) (12(NO$_3$), X = Cl). A 20-mL Schlenk tube was charged with **11**(NO_3) (0.140 g, 0.0419 mmol) and a magnetic stir bar. MeOH (5 mL) was added to the reaction vessel. A solution containing $NEt_4Cl\cdot H_2O$ (15.4 mg, 0.0840 mmol) in MeOH (3 mL) was added to the reaction vessel at 25 °C. A yellow solid precipitated immediately. After 15 min of stirring, the precipitate was isolated on a fritted glass filter, washed with MeOH and Et_2O, and dried under vacuum. The yellow solid was dissolved in CH_2Cl_2 (3 mL) and transferred to a Schlenk tube. Et_2O (7 mL) was added to the CH_2Cl_2 solution containing $[(PPh_3)Pt(AuPPh_3)_5(HgCl)_2](NO_3)$. After 10 min yellow crystals precipitated. The crystals were isolated on a fritted glass filter, washed with Et_2O, and dried under vacuum. The yield was 130 mg (94%) after recrystallization. **12**(NO_3), X = Cl, is soluble in CH_2Cl_2, chloroform, and acetone and insoluble in alcohols, saturated hydrocarbons, and Et_2O. ^{31}P NMR (CD_2Cl_2, 20 °C): δ 58.0 (sext with ^{195}Pt satellites, $^3J_{P-P}$ = 41.5 Hz, $J_{^{195}Pt-P}$ = 3042 Hz, $^2J_{^{199}Hg-P}$ unobserved, int = 1), 51.9 (d with ^{195}Pt satellites, $^3J_{P-P}$ = 41.5 Hz, $J_{^{199}Hg-P}$ = 479 Hz, $^2J_{^{195}Pt-P}$ = 386 Hz, int = 5). IR (KBr): $\nu(NO_3)$ 1341 cm^{-1}. The equivalent conductance (86.8 cm^2 mhos mol^{-1}) is indicative of a 1:1 electrolyte in CH_3CN solution. Anal. Calcd for $Au_5PtP_6C_{108}H_{90}Hg_2Cl_2NO_3\cdot CH_2Cl_2$: C, 38.82; H, 2.75; P, 5.51. Found: C, 38.31; H, 2.41; P, 5.70. **12**(NO_3), X = Br, was prepared in a fashion similar to that for **12**(NO_3), X = Cl, by using NEt_4Br in place of $NBu_4Cl(H_2O)$. Dark orange crystals were isolated, yield 95% after recrystallization. **12**(NO_3), X = Br, is soluble in CH_2Cl_2, chloroform, and acetone, and insoluble in alcohols, saturated hydrocarbons, and Et_2O. ^{31}P NMR (CD_2Cl_2, 20 °C): δ 58.8 (sext with ^{195}Pt satellites, $^3J_{P-P}$ = 40.3 Hz, $J_{^{195}Pt-P}$ 3043 Hz, $^2J_{^{199}Hg-P}$ unobserved, int = 1), 51.5 (d with ^{195}Pt satellites, $^3J_{P-P}$ = 40.3 Hz, $^2J_{^{199}Hg-P}$ = 473 Hz, $^2J_{^{195}Pt-P}$ = 385 Hz, int = 5). IR (KBr): $\nu(NO_3)$ 1341 cm^{-1}. The conductance (106.1 cm^2 mhos mol^{-1}) is indicative of a 1:1 electrolyte in CH_3CN solution. **12**(NO_3), X = I, was prepared in a fashion similar to that for **12**(NO_3), X = Cl, by using NBu_4I in place of $NBu_4Cl\cdot H_2O$. Red crystals were isolated, yield 93% after crystallization. **12**(NO_3), X = I, is soluble in CH_2Cl_2, chloroform, and acetone and insoluble in alcohols, saturated hydrocarbons, and Et_2O. ^{31}P NMR (CD_2Cl_2, 20 °C): δ 60.3 (sext with ^{195}Pt satellites, $^3J_{P-P}$ = 42.1 Hz, $^2J_{^{195}Pt-P}$ = 3036 Hz, $^2J_{^{199}Hg-P}$ unobserved, int = 1), 50.8 (d with ^{195}Pt satellites, $^3J_{P-P}$ = 42.1 Hz, $J_{^{199}Hg-P}$ = 414 Hz, $^2J_{^{195}Pt-P}$ = 385 Hz, int = 5). IR (KBr): $\nu(NO_3)$ 1341 cm^{-1}. The equivalent conductance (103.5 cm^2 mhos mol^{-1}) is indicative of a 1:1 electrolyte in CH_3CN solution.

Table I. Crystallographic Data for $[(CO)(PPh_3)Pt(AuPPh_3)_5](Cl)\cdot(CH_3CH_2)_2O$ and $[(PPh_3)Pt(AuPPh_3)_45(HgNO_3)_2](NO_3)\cdot 3CH_2Cl_2$

	8(Cl)·$(CH_3CH_2)_2O$	**11**$(NO_3)\cdot 3CH_2Cl_2$
Crystal Parameters and Measurement of Intensity Data		
space group	*C*2/*c* (No. 15)	$P\bar{1}$ (No. 2)
T, °C	−87	−114
cell params		
a, Å	35.91 (1)	14.18 (1)
b, Å	29.637 (7)	17.92 (1)
c, Å	26.025 (7)	22.91 (2)
α, deg		89.68 (7)
β, deg	132.62 (2)	84.80 (7)
γ, deg		69.18 (7)
V, Å^3	20383	5415
Z	8	2
calcd dens, g cm^{-3}	1.884	2.205
abs coeff, cm^{-1}	87.0	111.4
max, min transm factors	1.18, 0.69	1.36, 0.63
formula	$C_{113}H_{100}ClO_2P_6Au_5Pt$	$C_{111}H_{96}Cl_6N_3O_9P_6Au_5Hg_2Pt$
fw	2891.25	3595.67
Refinement by Full-Matrix Least Squares		
R^a	0.075	0.062
$R_w{}^a$	0.085	0.073

[a] The function minimized was $\sum w(|F_o| - |F_c|)^2$, where $w = 4F_o^2/\sigma^2(F_o)^2$. The unweighted and weighted residuals are defined as $R = \sum(||F_o| - |F_c||)/\sum|F_o|$ and $R_w = [(\sum w(|F_o| - |F_c|)^2)/(\sum w|F_o|^2)]^{1/2}$.

X-ray Structure Determinations. Collection and Reduction of X-ray Data. A summary of crystal is presented in Table I. Crystals of $[(CO)(PPh_3)Pt(AuPPh_3)_5](Cl)\cdot(CH_3CH_2)_2O$ (**8**(Cl)·$(CH_3CH_2)_2O$) and $[(PPh_3)Pt(AuPPh_3)_5(HgNO_3)_2](NO_3)\cdot 3CH_2Cl_2$ (**11**$(NO_3)\cdot 3CH_2Cl_2$) were coated with a viscous high molecular weight hydrocarbon and secured on a glass fiber with cooling in a cold N_2 stream on the diffractometer. The crystal classes and space groups were unambigously determined by the Enraf-Nonius CAD4 peak-search, centering, and indexing programs[17] and by successful solution and refinement of the structures (vide infra). The intensities of three standard reflections were measured every 1.5 h of X-ray exposure time during data collection, and no decay was noted for either crystal. The data were corrected for Lorentz, polarization, and background effects. An empirical absorption correction was applied by use of the program DIFABS.[18] All data were

(17) Schagen, J. D.; Straver, L.; van Meurs, F.; Williams, G. Enraf-Nonius Delft, Scientific Instruments Division, Delft, The Netherlands, 1988.

Table II. Positional Parameters and Their Estimated Standard Deviations for Core Atoms in $[(CO)(PPh_3)Pt(AuPPh_3)_5](Cl)\cdot(CH_3CH_2)_2O$[a]

atom	*x*	*y*	*z*	*B*, Å^2
Au2	0.20157 (7)	0.03326 (7)	0.0745 (1)	3.30 (9)
Au3	0.25917 (7)	0.07063 (7)	0.2194 (1)	2.61 (8)
Au4	0.31877 (7)	0.02000 (7)	0.20640 (9)	2.57 (8)
Au5	0.25772 (7)	−0.04994 (7)	0.10481 (9)	3.15 (9)
Au6	0.16408 (9)	−0.05926 (9)	0.0674 (1)	4.9 (1)
Pt	0.24102 (7)	−0.01648 (7)	0.18269 (9)	2.75 (8)
P1	0.2879 (5)	−0.0720 (5)	0.2675 (6)	3.5 (5)
P2	0.1584 (5)	0.0815 (6)	−0.0160 (7)	5.3 (7)
P3	0.2584 (5)	0.1391 (4)	0.2580 (7)	3.0 (5)
P4	0.3924 (4)	0.0471 (4)	0.2418 (6)	2.4 (5)
P5	0.2753 (5)	−0.0883 (5)	0.0476 (6)	3.6 (5)
P6	0.0882 (7)	−0.0940 (8)	−0.015 (1)	8 (1)
O1	0.163 (1)	0.003 (1)	0.193 (1)	2.5 (6)*
C1	0.188 (2)	−0.001 (1)	0.185 (2)	1.9 (5)*

[a] Counterion, solvent molecule, and phenyl group positional parameters are provided in the supplementary material. Starred *B* values are for atoms that were refined isotropically. *B* values for anisotropically refined atoms are given in the form of the isotropic equivalent thermal parameter defined as $(4/3)[a^2\beta(1,1) + b^2\beta(2,2) + c^2\beta(3,3) + ab(\cos\gamma)\beta(1,2) + ac(\cos\beta)\beta(1,3) + bc(\cos\alpha)\beta(2,3)]$.

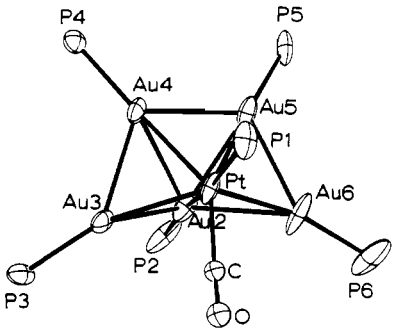

Figure 1. ORTEP drawing of the coordination core of **8**. Ellipsoids are drawn with 50% probability boundaries, and phenyl rings have been omitted for the sake of clarity.

collected by using an Enraf-Nonius CAD-4 diffractometer with controlling hardware and software,[17] and all calculations were performed by using the Molecular Structure Corp. TEXSAN crystallographic software package,[19] run on a Microvax 3 computer.

Solution and Refinement of the Structures. Both structures were solved by direct methods.[20,21] Full-matrix least-squares refinement and difference Fourier calculations were used to locate most of the remaining non-hydrogen atoms. In the case of $\mathbf{8}(Cl)\cdot(CH_3CH_2)_2O$ the chloride counterion was not located and five of the phenyl groups showed signs of disorder. The final difference Fourier map did not show any chemically meaningful features. In the case of $\mathbf{11}(NO_3)\cdot 3CH_2Cl_2$ the nitrate counterion was not located and several small peaks in the final difference Fourier map showed the presence of disordered solvent molecules. Disorder in ligands, solvent molecules, and counterions is common in structures of metal cluster complexes of this type and are not believed to significantly affect the molecular dimensions of the metal framework. The errors in the unit cell parameters for $\mathbf{11}(NO_3)\cdot CH_2Cl_2$ are larger than normal due to poor crystal quality, and since the TEXSAN programs do not allow for the error in the cell constants when calculating esd's of bond lengths and angles, these esd's should be increased by 1 part in 1000. The atomic scattering factors were taken from the usual tabulation,[22] and the effects of anomalous dispersion were included by F_c by

(18) Walker, N.; Stuart, D. *Acta. Crystallogr., Sect. A* **1983**, *A39*, 158.
(19) All calculations on the analysis of **2** were carried out with use of the Molecular Structure Corp. TEXSAN-TEXRAY Structure Analysis Package, version 2.1, 1985.
(20) MITHRIL (an integrated direct methods computer program, University of Glascow, Glascow, Scotland): Gilmore, C. J. *J. Appl. Crystallogr.* **1984**, *17*, 42.
(21) DIRDIF (direct methods for difference structures; an automatic procedure for phase extension and refinement of difference structure factors): Beurskens, P. T. Technical Report 1984/1; Crystallography Laboratory, Toernooiveld, 6525 Ed. Nijmegen, The Netherlands.
(22) Cromer, D. T.; Waber, J. T. In *International Tables for X-Ray Crystallography*; Kynoch: Birmingham, England, 1974; Vol. IV, Table 2.2.4.

Table III. Positional Parameters and Their Estimated Standard Deviations for Core Atoms in $[(PPh_3)Pt(AuPPh_3)_5(HgNO_3)_2](HgNO_3)_2](NO_3)\cdot 3CH_2Cl_2$[a]

atom	*x*	*y*	*z*	*B*, Å^2
Hg1	0.45348 (9)	0.41416 (8)	0.70795 (6)	2.28 (8)
Hg2	0.12471 (8)	0.51087 (8)	0.79641 (6)	1.90 (8)
Au1	0.24298 (8)	0.41222 (8)	0.69085 (5)	1.30 (7)
Au2	0.39501 (8)	0.27259 (8)	0.72870 (5)	1.42 (7)
Au3	0.19258 (8)	0.32781 (8)	0.79304 (5)	1.34 (7)
Au4	0.37099 (8)	0.27193 (8)	0.85180 (5)	1.41 (7)
Au5	0.28898 (8)	0.55079 (8)	0.74302 (5)	1.56 (8)
Pt	0.31616 (8)	0.41021 (7)	0.79336 (5)	1.01 (7)
P1	0.1633 (5)	0.4309 (5)	0.6069 (3)	1.5 (5)
P2	0.5008 (6)	0.1674 (6)	0.6710 (4)	2.4 (6)
P3	0.0540 (5)	0.2929 (5)	0.8110 (3)	1.6 (5)
P4	0.4278 (5)	0.1609 (5)	0.9080 (3)	1.5 (5)
P5	0.2820 (6)	0.6736 (5)	0.7133 (3)	1.9 (5)
P6	0.3722 (5)	0.4447 (5)	0.8758 (3)	1.6 (5)
O13	0.553 (2)	0.382 (2)	0.602 (1)	4.9 (6)*
O14	0.709 (2)	0.371 (2)	0.597 (1)	3.6 (5)*
N22	−0.051 (2)	0.640 (2)	0.849 (1)	4.1 (7)*
N12	0.625 (2)	0.388 (2)	0.626 (1)	3.1 (6)*
O21	−0.041 (2)	0.601 (2)	0.803 (1)	5.8 (7)*
O23	0.016 (3)	0.614 (3)	0.879 (2)	12 (1)*
O24	−0.128 (2)	0.698 (2)	0.868 (1)	7.0 (8)*
O11	0.613 (2)	0.411 (2)	0.678 (1)	4.4 (6)*

[a] See footnote in Table II.

Table IV. Selected Bond Lengths (Å) and Bond Angles (deg) with Esd's for the Cluster Core of **8**

Bond Lengths			
Pt–Au2	2.590 (3)	Au2–Au3	3.028 (3)
Pt–Au3	2.676 (3)	Au2–Au4	3.176 (3)
Pt–Au4	2.648 (4)	Au2–Au5	2.935 (3)
Pt–Au5	2.664 (4)	Au2–Au6	3.005 (4)
Pt–Au6	2.649 (3)	Au3–Au4	2.816 (4)
Pt–P1	2.32 (1)	Au4–Au5	2.871 (3)
Pt–C1	1.99 (6)	Au5–Au6	2.811 (5)
Au2–P2	2.25 (2)	Au5–P5	2.28 (2)
Au3–P3	2.27 (2)	Au6–P6	2.27 (2)
Au4–P4	2.28 (2)	C1–O1	1.05 (8)

Bond Angles			
Au2–Pt–Au3	70.2 (1)	Au4–Pt–C1	141 (1)
Au2–Pt–Au4	74.6 (1)	Au5–Pt–Au6	63.9 (1)
Au2–Pt–Au5	67.9 (1)	Au5–Pt–P1	93.9 (5)
Au2–Pt–Au6	70.0 (1)	Au5–Pt–C1	145 (1)
Au2–Pt–P1	161.5 (5)	Au6–Pt–P1	105.5 (3)
Au2–Pt–C1	94 (1)	Au6–Pt–C1	82 (1)
Au3–Pt–Au4	63.9 (1)	P1–Pt–C1	103 (1)
Au3–Pt–Au5	120.3 (1)	Pt–Au2–P2	169.3 (6)
Au3–Pt–Au6	132.96 (9)	Pt–Au3–P3	161.1 (6)
Au3–Pt–P1	120.0 (3)	Pt–Au4–P4	172.1 (3)
Au3–Pt–C1	77 (1)	Pt–Au5–P5	171.4 (4)
Au4–Pt–Au5	65.4 (1)	Pt–Au6–P6	161.8 (8)
Au4–Pt–Au6	125.9 (1)	Pt–C1–O1	171 (4)
Au4–Pt–P1	92.5 (5)		

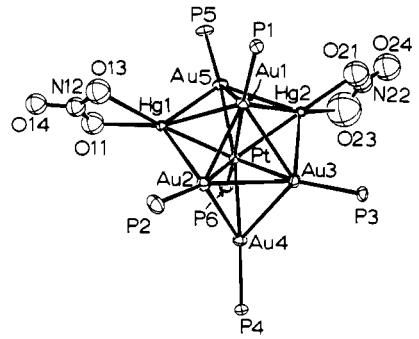

Figure 2. ORTEP drawing of the coordination core of **11**. Ellipsoids are drawn with 50% probability boundaries, and phenyl rings have been omitted for the sake of clarity.

using Cromer and Ibers's values of $\Delta f'$ and $\Delta f''$.[23] The metal and phosphorus atoms in both structures were refined with anisotropic

Table V. Selected Bond Lengths (Å) and Bond Angles (deg) with Esd's for the Cluster Core of **11**

Bond Lengths			
Pt-Au1	2.647 (3)	Au1-Au3	2.951 (3)
Pt-Au2	2.703 (3)	Au1-Au5	3.056 (3)
Pt-Au3	2.663 (3)	Au2-Au3	2.936 (3)
Pt-Au4	2.705 (3)	Au2-Au4	2.811 (3)
Pt-Au5	2.680 (3)	Au3-Au4	2.831 (3)
Pt-Hg1	2.651 (3)	Au1-P1	2.282 (8)
Pt-Hg2	2.667 (3)	Au2-P2	2.282 (9)
Hg1-Au1	3.057 (3)	Au3-P3	2.268 (9)
Hg1-Au2	2.959 (3)	Au4-P4	2.299 (9)
Hg1-Au5	2.775 (4)	Au5-P5	2.27 (1)
Hg2-Au1	2.999 (4)	Pt-P6	2.284 (9)
Hg2-Au3	3.072 (3)	N12-O11	1.24 (4)
Hg2-Au5	2.844 (3)	N12-O13	1.24 (4)
Hg1-O11	2.28 (3)	N12-O14	1.25 (4)
Hg1-O13	2.66 (3)	N22-O21	1.22 (5)
Hg2-O21	2.32 (3)	N22-O23	1.20 (6)
Hg2-O23	2.62 (4)	N22-O24	1.26 (4)
Au1-Au2	2.853 (3)		
Bond Angles			
Hg1-Pt-Hg2	120.97 (9)	Au4-Pt-Au5	170.15 (7)
Hg1-Pt-Au1	70.47 (8)	Hg2-Pt-Au1	68.70 (9)
Hg1-Pt-Au2	67.09 (9)	Hg2-Pt-Au2	124.99 (9)
Hg1-Pt-Au3	126.92 (8)	Hg2-Pt-Au3	70.39 (8)
Hg1-Pt-Au4	113.43 (9)	Hg2-Pt-Au4	122.80 (9)
Hg1-Pt-Au5	62.73 (9)	Hg2-Pt-Au5	64.27 (8)
Hg1-Pt-P6	104.1 (2)	Hg2-Pt-P6	103.6 (2)
Pt-Hg1-O11	149.8 (7)	Pt-Hg2-O21	177.4 (8)
Pt-Hg1-O13	156.0 (8)	Pt-Hg2-O23	129 (1)
Au1-Hg1-O11	155.3 (7)	Au1-Hg2-O21	123.3 (8)
Au1-Hg1-O13	104.6 (7)	Au1-Hg2-O23	172 (1)
Pt-Au-P1	171.9 (2)	Hg1-O11-N12	103 (2)
Pt-Au2-P2	163.6 (3)	Hg1-O13-N12	85 (2)
Pt-Au3-P3	161.1 (2)	Hg2-O21-N22	105 (2)
Pt-Au4-P4	173.2 (2)	Hg2-O23-N22	91 (3)
Pt-Au5-P5	169.6 (2)	O11-N12-O13	120 (3)
Au1-Pt-P6	164.0 (2)	O21-N22-O23	115 (3)

thermal parameters. The phenyl carbon atoms in both structures were refined as rigid groups. The positions of the hydrogen atoms in the PPh_3 ligands were not included in the structure factor calculations of either structure. The final positional and thermal parameters of the refined atoms within the coordination core for **8**(Cl)·$(CH_3CH_2)_2O$) and **11**·(NO_3)·$3CH_2Cl_2$ are given in Tables II and III, respectively. ORTEP drawings of the cluster cores for both complexes including the labeling schemes are shown in Figures 1 and 2. Tables IV and V list selected distances and angles within the cluster cores of both complexes. A complete listing of thermal parameters, positional parameters, distances, angles, least-squares planes, and structure factor amplitudes are included as supplementary material.[24]

Results

The transformations observed in this study are summarized in Schemes I and II. All of the compounds listed were isolated as solids in high yield.

The reaction of the (μ_3-oxo)tris(triphenylphosphine)gold(I) cation, $[(AuPPh_3)_3O]BF_4$, with $Pt(PPh_3)_2(C_2H_4)$ followed by treatment with $Au(PPh_3)NO_3$ and NBu_4I gives the new $PtAu_4$ cluster **4**. Reaction of **4** with PPh_3 gives the new $PtAu_3$ cluster **1** with $AuPPh_3I$ as a side product. This reaction can be viewed as the PPh_3-promoted reductive elimination of $Au(PPh_3)I$. Compounds **1** and **4** are 16-electron clusters and therefore are reactive with nucleophiles. Thus, reaction of **1** with CO gives the 18-electron carbonyl adduct **2** and reaction of **4** with the diphosphine dppe gives the 18-electron cluster **5**. Compound **5** is very stable, but I^- can be removed by reaction with $TlPF_6$, giving the 16-electron cluster **6** and TlI. The $PtAu_3$ cluster **1** also reacts with the electrophile $AuPPh_3^+$ to give the new 16-electron adduct **3**. Complexes **3**–**6** are the first $PtAu_4$ clusters synthesized in this series. The reaction of **1** with 1 equiv of $[(AuPPh_3)_3O]BF_4$ gives the known 16-electron $PtAu_6$ cluster **7** in quantitative yield. The net reaction is the addition of $[Au(PPh_3)]_3^+$ with loss of $OPPh_3$. The reaction of **7** with the nucleophile CO gives the 18-electron adduct $[(CO)(PPh_3)Pt(AuPPh_3)_6]^{2+}$, as reported previously.[3] This complex is converted into the $PtAu_5$ cluster **8** upon the addition of 1 equiv of PPh_3 and loss of $[Au(PPh_3)_2]^+$. Although these last two reactions have been reported previously,[3] complex **8** was not structurally characterized. The X-ray crystal structure of **8**·(Cl)·$(CH_3CH_2)_2O$) is reported here and discussed in the next section (see Figure 1). These transformations are shown in Scheme I.

The reaction of **7** with other nucleophiles X^- (X = Br, I, CN) and phosphite ligands gave the 18-electron adducts **9** and **10**, respectively. The novel oxidative-addition reaction of $(HgNO_3)_2$ to **7** gives the 18-electron $PtAu_5Hg_2$ cluster **11**. The X-ray crystal structure of this unusual compound is reported here and is discussed in the next section (see Figure 2). These transformations are shown in Scheme II.

The spectroscopic and crystallographic data obtained for the new compounds are given in the Experimental Section and are discussed in the next section.

Discussion

Synthesis and Spectroscopic Characterization of the Clusters. Values of NMR chemical shifts and coupling constants are given in the Experimental Section and therefore are not generally repeated in this section. Refer to Schemes I and II for the formulation of the compounds and for a summary of their transformations. Complex **1** was synthesized in high yield and isolated in pure form by the reaction of **4** with 1 equivalent of PPh_3 in acetone solution. The byproduct $Au(PPh_3)I$, which was identified by ^{31}P NMR spectroscopy, precipitated during the course of the reaction. Complex **1** was also synthesized by stirring solutions containing equimolar amounts of $Pt(PPh_3)_2(C_2H_4)$ and $[(AuPPh_3)_3O]BF_4$ at 0 °C in acetone, THF, or CH_2Cl_2 solvent. The resulting reaction product was always contaminated with **7**. Separation of the reaction mixtures containing **1** and **7** was not possible.

The ^{31}P NMR spectrum (20 °C, CD_2Cl_2) of **1** showed two resonances at δ 60.2 and 47.3 with a relative intensity of 2:3. The peak assigned to the PPh_3 ligands bound to the Pt atom (δ 60.2) appeared as a quartet with ^{195}Pt satellites. The upfield resonance (δ 47.3) assigned to the $Au(PPh_3)$ ligands appeared as a triplet with ^{195}Pt satellites. The ^{31}P NMR spectrum of **1** is indicative of fluxional behavior but is consistent with its formulation. Fluxional NMR behavior is generally observed with Pt–Au and Au clusters.[10] ^1H NMR spectroscopy showed no evidence for hydride ligands.

Positive ion FABMS analysis of **1**(PF_6) gave a spectrum with well-resolved peaks. An analysis of the isotopic ion distribution pattern for the highest mass peak gave a most abundant mass ion of m/e 2097.5, which corresponded to the ion $[(PPh_3)_2Pt(AuPPh_3)_3]^+$. A complete analysis of the fragmentation pattern suggested that the neutral compound was $[(PPh_3)_2Pt(AuPPh_3)_3](PF_6)$. In agreement with this formulation, the conductance of **1** in CH_3CN showed it to be a 1:1 electrolyte, for both BF_4^- and PF_6^- salts.

Complex **2** was prepared by the exposure of a solution of **1** to 1 atm of CO with use of CH_2Cl_2 as solvent. The characterization data are consistent with the formulation of **2** as the carbonyl adduct of **1** with two PPh_3 ligands and one CO ligand bonded to the Pt atom. This reaction is analogous to the reaction of **7** with CO, which yielded $[(CO)(PPh_3)Pt(AuPPh_3)_6](NO_3)_2$.[3] The ^{31}P NMR spectrum (20 °C, CD_2Cl_2) of **2** showed two resonances at δ 45.6 and 32.9 with a relative intensity of 3:2. The peak assigned to the $Au(PPh_3)$ ligands (δ 45.6) appeared as a triplet with ^{195}Pt satellites. The upfield resonance (δ 32.9) assigned to the $Pt(PPh_3)$ ligands bonded to Pt appeared as a quartet with ^{195}Pt satellites. The ^{31}P NMR spectrum of **2** is indicative of fluxional behavior but is in agreement with its formulation. ^1H NMR spectroscopy showed no evidence for hydride ligands.

The ^{13}C NMR solution spectrum (CD_2Cl_2, 20 °C) of the ^{13}CO analogue of **2** consisted of a quartet at δ 198.3 ($^3J_{^{13}C-P}$ = 15.6 Hz)

(23) Cromer, D. T. In *International Tables for X-Ray Crystallography*; Kynoch: Birmingham, England, 1974; Vol. IV, Table 2.3.1.

(24) See paragraph at the end of paper regarding supplementary material.

with ^{195}Pt satellites. The quartet resonances are broadened, suggesting unresolved coupling to the phosphorus atoms bound to the Pt. The observation that the ^{13}C–P coupling constant is larger for the more distant Au*P*Ph$_3$ than for the Pt*P*Ph$_3$ has also been noted for (CO)(PPh$_3$)Pt(AuPPh$_3$)$_6$ and for **8**.[3] The IR spectrum (KBr) of **3** displayed a ν(CO) absorption at 1974 cm^{-1}, which is consistent with a terminal bound metal carbonyl. The absorption shifted to lower energy (1924 cm^{-1}) when **2** was synthesized with 99% ^{13}CO. In agreement with the formulation of **2** as [(CO)(PPh$_3$)$_2$Pt(AuPPh$_3$)$_3$]$^+$, the conductance of **2**(PF$_6$) in CH$_3$CN solution showed it to be a 1:1 electrolyte.

Compound **3** was synthesized by the addition of 1 equiv of [Au(PPh$_3$)]$^+$ as the nitrate salt to **1** in acetone solution. The ^{31}P NMR spectrum (20 °C, CD$_2$Cl$_2$) of **3** showed two resonances at δ 53.9 and 44.0 with a relative intensity of 1:2. The peak assigned to the PPh$_3$ ligands bound to the Pt atom (δ 53.9) appeared as a pentet with ^{195}Pt satellites. The upfield resonance (δ 44.0) assigned to the Au(PPh$_3$) ligands appeared as a triplet with ^{195}Pt satellites. The ^{31}P NMR spectrum of **3** indicates fluxional behavior at 20 °C, and the resonances broadened as the temperature was lowered. At −100 °C the spectrum began to freeze out into four resonances too broad to show P–P coupling with relative intensities of 2:2:1:1. Each resonance showed a well-resolved ^{195}Pt–P coupling (see Experimental Section). One of the resonances with intensity of 2 is assigned to the PPh$_3$ ligands bound to the Pt because the ^{195}Pt–P coupling constant was large (3271 Hz), while the others were typical of two-bond coupling (226–504 Hz). 2D NMR experiments are needed to sort out P–P coupling before any suggestion of the geometry in solution can be made. This work is in progress. ^{1}H NMR spectroscopy showed no evidence for hydride ligands. Positive ion FABMS analysis of **3** gave a spectrum with well-resolved peaks. An analysis of the isotopic ion distribution pattern for the highest mass peak gave a most abundant mass ion of *m/e* 2701.3, which corresponded to the ion pair [(PPh$_3$)$_2$Pt(AuPPh$_3$)$_4$(PF$_6$)]$^+$. A complete analysis of the fragmentation pattern suggested that the neutral compound was [(PPh$_3$)$_2$Pt(AuPPh$_3$)$_4$](PF$_6$)$_2$. In agreement with this formulation, the conductance of **3**(PF$_6$)$_2$ in CH$_3$CN solution showed it to be a 2:1 electrolyte.

Compound **4** was synthesized in one pot from the reaction of Pt(PPh$_3$)$_2$(C$_2$H$_4$) and [(AuPPh$_3$)$_2$O]BF$_4$ without isolation of any intermediates. Complex **4** was isolated as PF$_6^-$ and BF$_4^-$ salts, and both showed identical NMR spectra. The ^{31}P NMR spectrum (20 °C, CD$_2$Cl$_2$) of **4** showed two resonances at 57.6 and 43.4 with a relative intensity of 1:4. The peak assigned to the PPh$_3$ ligand bound to the Pt atom (δ 57.6) appeared as a pentet with ^{195}Pt satellites. The upfield resonance (δ 43.4) assigned to the Au(PPh$_3$) ligands appeared as a doublet with ^{195}Pt satellites. The ^{31}P NMR spectrum of **4** is indicative of fluxional behavior but is in agreement with its formulation. ^{1}H NMR spectroscopy showed no evidence for hydride ligands.

Positive ion FABMS analysis of **4**(BF$_4$) gave a spectrum with well-resolved peaks. An analysis of the isotopic ion distribution pattern for the highest mass peak gave a most abundant mass ion of *m/e* 2421.2, which corresponds to the ion [(I)(PPh$_3$)Pt(AuPPh$_3$)$_4$]$^+$. A complete analysis of the fragmentation pattern suggested that the neutral compound was [(I)(PPh$_3$)Pt(AuPPh$_3$)$_4$](BF$_4$). In agreement with this formulation, the conductance of **4** in CH$_3$CN solution showed it to be a 1:1 electrolyte, whether the counterion was BF$_4^-$ or PF$_6^-$. These data provide strong support for the presence of a Pt–I bond.

Complex **5** was synthesized by the reaction of **4** with 1 equiv of dppe in CH$_2$Cl$_2$ solution. The ^{31}P NMR spectrum (20 *C*, 1,1,2-trichloroethane) of **5** showed two broad resonances at δ 76.6 and 50.7 with a relative intensity of 1:2. Both of these resonances had broad ^{195}Pt satellites. The spectrum sharpened upon increasing the temperature, and at 75 °C the high-temperature-limiting spectrum was reached. The ^{31}P NMR spectrum at this temperature showed signals at approximately the same positions. The peak assigned to the dppe ligand bound in a chelated fashion to the Pt atom (δ 76.6) appeared as a pentet with ^{195}Pt satellites. The upfield resonance (δ 50.7) assigned to the Au(PPh$_3$) ligands appeared as a triplet with ^{195}Pt satellites. The observation of fluxional behavior at room temperature suggested that low-temperature experiments should be carried out. The ^{31}P spectrum at −100 °C gave sharp signals, indicating that the low-temperature limit was reached. This spectrum was very complex and showed a number of multiplets that could not be easily assigned. In addition, it appeared that two isomers of the complex were present. A complete analysis of this spectrum using 2D methods is in progress. ^{1}H NMR spectroscopy showed no evidence for hydride ligands. The NMR data are in agreement with the formulation of **5** but a determination of the solution geometry could not be made. In agreement with this formulation, the conductance of **5**(PF$_6$) in CH$_3$CN solvent showed it to be a 1:1 electrolyte. As with **4**, these data provide convincing evidence that the iodide is strongly bound to Pt.

Complex **6** was synthesized by the reaction of **5** with TlPF$_6$ in CH$_2$Cl$_2$/CH$_3$CN solution. The byproduct TlI precipitated during the course of the reaction. The ^{31}P NMR spectrum (20 °C, CD$_2$Cl$_2$) of **6** showed two resonances at δ 60.2 and 47.3 with a relative intensity of 1:2. The peak assigned to the dppe ligand bound to the Pt atom (δ 82.2) appeared as a pentet with ^{195}Pt satellites. The upfield resonance (δ 50.7) assigned to the Au(PPh$_3$) ligands appeared as a triplet with ^{195}Pt satellites. The ^{31}P NMR spectrum of **6** is indicative of fluxional behavior but is in agreement with its formulation. The ^{1}H NMR spectrum of **6** showed resonances at δ 7.8–6.8 and 2.41 with a relative intensity of 20:1. The multiplets assigned to the phenyl protons appeared in the region 7.8–6.8 ppm. The upfield resonance (δ 2.41) assigned to the protons on the ethyl backbone of the dppe ligand appeared as a multiplet. No evidence for hydride ligands was present in the ^{1}H NMR spectrum. Positive ion FABMS analysis of **6** gave a spectrum with well-resolved peaks. An analysis of the isotopic ion distribution pattern for the highest mass peak gave a most abundant mass ion of *m/e* 2575.0, which corresponded to the ion pair [(dppe)Pt(AuPPh$_3$)$_4$(PF$_6$)]$^+$. A complete analysis of the fragmentation pattern suggested that the neutral compound was [(dppe)Pt(AuPPh$_3$)$_4$](PF$_6$)$_2$. In agreement with this formulation, the conductance of **6**(PF$_6$)$_2$ in CH$_3$CN solution showed it to be a 2:1 electrolyte.

Complex **9**, X = I, was synthesized as the nitrate salt by the reaction of **7** with 1 equiv of NBu$_4$I in acetone solution. It is important to note that the formation of **9**, X = I, was dependent on solvent, as the reaction did not yield the desired product with use of CH$_2$Cl$_2$. The ^{31}P NMR spectrum (20 °C, CD$_2$Cl$_2$) of isolated **9**, X = I, showed two resonances at δ 56.8 and 45.4 with a relative intensity of 1:6 indicative of fluxional behavior. The peak assigned to the PPh$_3$ ligand bound to the Pt atom (δ 56.8) appeared as a septet with ^{195}Pt satellites. The upfield resonance (δ 45.4) assigned to the Au(PPh$_3$) ligands appeared as a doublet with ^{195}Pt satellites. Upon lowering of the temperature, the peaks broadened and then sharpened up at about −100 °C. At this temperature the spectrum was complex and could not be easily assigned. An understanding of this spectrum and its possible suggestion of the cluster geometry must wait until a 2D experiment can be run. The ^{31}P NMR spectrum run at 20 °C of the crude reaction mixture showed only the formation of **9**, X = I, in quantitative yield. The isolation of a quantitative yield and the ^{31}P NMR spectroscopic data suggest that **9**, X = I, is an adduct of **7** in which the iodine atom is bound to Pt. The ^{31}P NMR chemical shifts and coupling constants for the starting compound **7** and for **9**, X = Br, and **9**, X = I, are quite different although the coupling patterns are similar as expected. These data are summarized in Table VI. If the I$^-$ and Br$^-$ ions were present only as counterions, this would not be the case. The poor solubility of **9**, X = I, in organic solvents such as acetone, MeOH, and CH$_3$CN precluded the measurement of its conductance. This poor solubility contrasts with other Pt–Au cluster compounds synthesized in this laboratory and may result because the iodide ligand is bound to Pt. The IR (KBr) spectrum of **9**, X = I, showed no absorption at 1345 cm^{-1}, which is attributed to the presence of unbound NO$_3^-$. The bromide analogue, **9**, X = Br, was synthesized by the reaction of **7** with 1 equiv of NBu$_4$Br in acetone

Table VI. ^{31}P NMR Data for Adducts of $[(PPh_3)Pt(Au(PPh_3)_6]^{2+}$ (**7**)[a]

compd	chem shift, ppm		P–X coupling const, Hz	
	$(PPh_3)Pt$[b]	$(PPh_3)Au$[c]	X = P	X = Pt
$[(PPh_3)Pt(AuPPh_3)_6]^{2+}$	62.3		30	3766
		50.3	30	413
$[(CO)(PPh_3)Pt(AuPPh_3)_6]^{2+}$	47.3		28	2469
		48.0	28	385
$[(CN)(PPh_3)Pt(AuPPh_3)_6]^{+}$	59.2		42	2222
		44.6	42	415
$[(Br)(PPh_3)Pt(AuPPh_3)_6]^{+}$	60.8		32	3667
		48.3	32	439
$[(I)(PPh_3)Pt(AuPPh_3)_6]^{+}$	56.8		37	3379
		45.4	37	493

[a] The NMR data are invariant for counterions NO_3^-, BF_4^-, and PF_6^-. [b] Septet pattern due to P–P coupling. [c] Doublet pattern due to P–P coupling.

solution. The analysis of the characterization and properties of **9**, X = Br, are similar to that of the iodide analogue. The cyanide analogue, **9**, X = CN, was synthesized as the nitrate salt by the reaction of **7** with 1 equiv of KCN in methanol solution. The characterization data are consistent with the formulation of **9**, X = CN, as the CN adduct of **7** with one PPh_3 ligand and one CN ligand bonded to the Pt atom. The ^{31}P NMR spectrum (20 °C, CD_2Cl_2) of **9**, X = CN, showed two resonances at δ 59.2 and 44.6 with a relative intensity of 1:6 indicative of fluxional behavior. The chemical shifts and coupling constants are shown in Table VI. In agreement with the formulation of **9**, X = CN, as $[(CN)(PPh_3)Pt(AuPPh_3)_6]^+$, the conductance of the nitrate salt in CH_3CN solution showed it to be a 1:1 electrolyte. The IR (KBr) spectrum showed absorptions at 2073 cm^{-1}, due to ν(C–N) of the CN ligand bonded to Pt, and at 1341 cm^{-1}, attributed to the presence of unbound NO_3^-, respectively.

Complex **10a** was synthesized by the addition of an excess of $P(OCH_3)_3$ to a CH_2Cl_2 solution containing **7**. The characterization data are consistent with the formulation of **10a** as a derivative of **7** where the PPh_3 ligand bonded to Pt has been replaced by two $P(OCH_3)_3$ ligands. The ^{31}P NMR spectrum (20 °C, CD_2Cl_2) of **10a** showed two resonances at δ 157.0 and 49.0 with a relative intensity of 1:3 and was indicative of fluxional behavior. The peak assigned to the $P(OCH_3)$ ligands bound to the Pt atom (δ 157.0) appeared as a septet with ^{195}Pt satellites ($J_{^{195}Pt-P}$ = 4107 Hz). The large P–Pt coupling constant requires the $P(OCH_3)_3$ ligands to be directly bonded to Pt. There was not any evidence for the substitution of $P(OCH_3)_3$ for PPh_3 ligands bound to gold. The upfield resonance (δ 49.0) assigned to the $Au(PPh_3)$ ligands appeared as a triplet with ^{195}Pt satellites. At −100 °C the spectrum became complicated as the frozen out limit was reached. As with the other complexes discussed above, the low-temperature spectrum could not be easily assigned and it is expected that a 2D experiment will help. This experiment is planned for the future. The ^1H NMR spectrum of **10a** showed resonances at δ 7.4–6.7 and 3.33 with a relative intensity of 5:1. The multiplets assigned to the phenyl protons appeared in the region 7.4–6.7 ppm. The upfield resonance (δ 3.33) assigned to the protons of the $P(OCH_3)$ ligands appeared as a multiplet. No evidence for hydride ligands was present in the ^1H NMR spectrum. In agreement with the formulation of **10a** as $[(P(OCH_3)_3)_2Pt(AuPPh_3)_6]^{2+}$, the conductance of **10a**$(NO_3)_2$ in CH_3CN solution showed it to be a 2:1 electrolyte. Complex **10b** was synthesized by the reaction of **7** with an excess of $P(OCH_2)_3CCH_3$ in CH_2Cl_2 solution. The properties and spectroscopic characterization of **10b** are similar to those of **10a**.

Complex **11** was synthesized by the reaction of **7** with 1 equiv of $Hg_2(NO_3)_2(H_2O)_2$ in methanol solution. The ^{31}P NMR spectrum (20 °C, CD_2Cl_2) of **11** showed two resonances at δ 54.9 and 53.1 with a relative intensity of 1:5. The peak assigned to the PPh_3 ligand bound to the Pt atom (δ 54.9) appeared as a sextet with ^{195}Pt satellites ($J_{^{195}Pt-P}$ = 3258 Hz). The ^{199}Hg satellites were not observed (intensity too low). The upfield resonance assigned to the $Au(PPh_3)$ ligands appeared as a doublet with ^{195}Pt and ^{199}Hg satellites ($^2J_{^{195}Pt-P}$ = 390 Hz, $J_{^{199}Hg-P}$ = 604 Hz). The ^{31}P NMR spectrum of **11** is indicative of fluxional behavior in solution but is entirely consistent with its formulation as a Pt-centered cluster with five peripheral $AuPPh_3$ and two $Hg(NO_3)$ units bonded to Pt via M–M bonds. ^1H NMR spectroscopy showed no evidence for hydride ligands. Positive ion FABMS analysis of **11**(NO_3) gave a spectrum with well-resolved peaks. An analysis of the isotopic ion distribution pattern for the highest mass peak gave a most abundant mass ion of m/e 3279.2, which corresponded to the ion $[(PPh_3)Pt(AuPPh_3)_5(HgNO_3)]^+$. A complete analysis of the fragmentation pattern suggested that the neutral compound was $[(PPh_3)Pt(AuPPh_3)_5(HgNO_3)_2](NO_3)$. **11**$(NO_3)$ showed a conductance of 155.5 cm^2 mhos mol^{-1} in CH_3CN solution, which is higher than normally observed for other +1 charged complexes of this general class (normal range 80–120 cm^2 mhos mol^{-1}). It is presumed that there is some dissociation of the NO_3^- ligands bonded to Hg in solution. The IR (KBr) spectrum of **11**(NO_3) showed absorptions at 1341 and 1255 cm^{-1}, which are due to unbound and bound nitrate, respectively. In order to fully investigate this novel compound, a single-crystal X-ray analysis was carried out (vide infra). The results of this analysis confirm the formulation as **11**(NO_3) in the solid state.

Complex **12**, X = Cl, was synthesized by the addition of 2 equiv of Cl^- as the NEt_4 salt to a MeOH solution of **11**. The ^{31}P NMR spectrum (20 °C, CD_2Cl_2) of **12**, X = Cl, showed two resonances at δ 58.0 and 51.9 with a relative intensity of 1:5 indicative of fluxional behavior. The peak assigned to the PPh_3 ligand bound to the Pt atom (δ 58.0) appeared as a sextet with ^{195}Pt satellites ($J_{^{195}Pt-P}$ = 3042 Hz). The ^{199}Hg satellites were not observed (intensity too low). The upfield resonance (δ 51.9) assigned to the $Au(PPh_3)$ ligands appeared as a doublet with ^{195}Pt and ^{199}Hg satellites ($^2J_{^{195}Pt-P}$ = 386 Hz, $J_{^{199}Hg-P}$ = 479 Hz). In agreement with the formulation of **12**, X = Cl, as $[(PPh_3)Pt(AuPPh_3)_5(HgCl)_2]^+$, its conductance in CH_3CN solution showed it to be a 1:1 electrolyte. The IR (KBr) spectrum showed an absorption at 1341 cm^{-1}, which is attributed to the presence of unbound NO_3^-. **12**, X = Br and I, were prepared in a fashion similar to that of **12**, X = Cl, with NBu_4X in place of NBu_4Cl. The properties and characterization data of these compounds are similar to those of **12**, X = Cl.

Crystal Structure of $[(CO)(PPh_3)Pt(AuPPh_3)_5]Cl\cdot(CH_3CH_2)_2O$ (8(Cl)·$(CH_3CH_2)_2O$). In the solid state this cluster ion has a central platinum atom bonded to give peripheral $AuPPh_3$ units, one PPh_3, and one CO ligand to give a seven-coordinate platinum atom. This general formulation is confirmed by ^{31}P and ^{13}C NMR, IR, conductivity, and FABMS data,[3] although the fluxionality in the NMR spectrum precludes a determination of geometry. The chloride counterion was not located in the X-ray analysis; however, conductivity measurements confirmed the +1 charge on **8**. The structure of the coordination core is shown in Figure 1, and selected distances and angles are shown in Table IV.

The structure of **8** is closely related to that of $[(CO)(PPh_3)Pt(AuPPh_3)_6]^{2+}$,[3] in that both can be described as fragments of a Pt-centered icosahedron, as illustrated in Figure 3. This figure shows the usefulness of describing these structures as icosahedral fragments and clearly shows the geometrical relationships to the larger 18-electron Pt-centered clusters $[(PPh_3)Pt(AuPPh_3)_5(HgNO_3)_2]^+$ (**11**), $[(CO)Pt(AuPPh_3)_8]^{2+}$,[6] and $[(CO)Pt(AuPPh_3)_8(AgNO_3)]^{3+}$.[7] The metal positions in all of these clusters closely approximate idealized centered icosahedral positions. Centered clusters that have the 18-electron configuration are expected to have such a spheroidal geometry (vide infra),[3,6,7,11,12,25] and the centered icosahedron is well established for small gold[26] and silver–gold clusters.[27] The platinum-centered

(25) Hall, K. P.; Gilmour, D. I.; Mingos, D. M. P. *J. Organomet. Chem.* **1984**, *268*, 275.
(26) Briant, C. E.; Theobald, B. R. C.; White, J. W.; Bell, L. K.; Mingos, D. M. P.; Welch, A. J. *J. Chem. Soc., Chem. Commun.* **1981**, 201.
(27) Teo, B. K.; Zhang, H.; Shi, X. *Inorg. Chem.* **1990**, *29*, 2083. Teo, B. K.; Keating, K. *J. Am. Chem. Soc.* **1984**, *106*, 2224. Teo, B. K.; Hong, M.; Zhang, H.; Huang, D.; Shi, X. *J. Chem. Soc., Chem. Commun.* **1988**, 204.

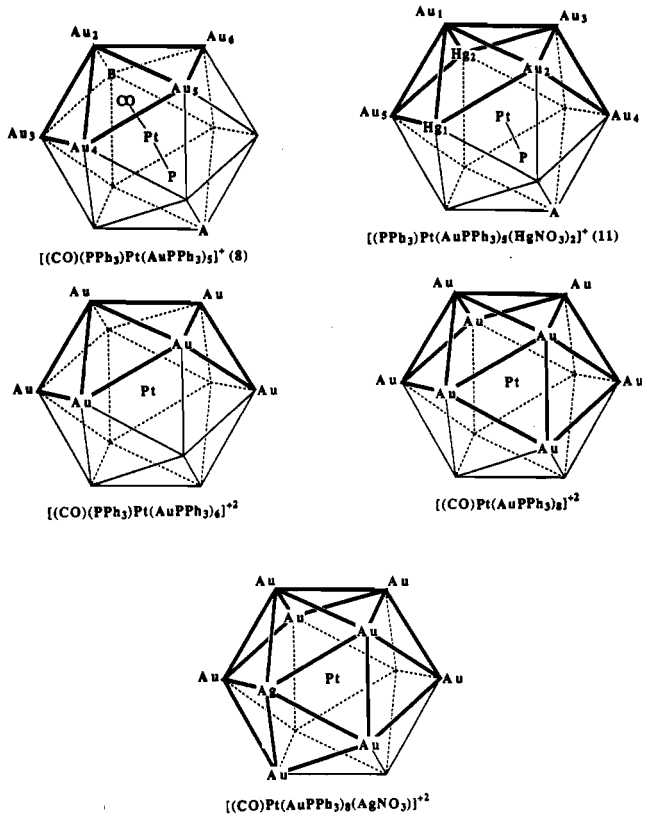

Figure 3. Metal core geometries of several 18-electron Pt-centered clusters shown as fragments of the centered icosahedron. The darkened lines represent bonding interactions between metal atoms. The central Pt atom is bonded to all of the peripheral metals, but these bonds are not shown for the sake of carity.

gold clusters that have 16-electron configurations such as **7**[3] and $[Pt(AuPPh_3)_8]^{2+}$[6] have a toroidal geometry and therefore cannot be described as fragments of a centered icosahedron (vide infra).

In **8** the CO and Pt-bound PPh_3 ligands occupy adjacent positions (C1–Pt–P1 = 103 (1)°) and are positioned in the directions of the icosahedron vertices B and A, respectively, as shown in Figure 3. The Au–Pt distances in **8** (average 2.645 Å, range 2.590 (3)–2.676 (3) Å) are within the range of values observed in other Au–Pt clusters containing primarily phosphine ligands (for example, average 2.678 in **7**,[3] 2.687 in $[(CO)(PPh_3)Pt(AuPPh_3)_6]^{2+}$,[3] and 2.635 Å in $[Pt(AuPPh_3)_8]^{2+}$[6]). The distance between Pt and the Au atom trans to the phosphine attached to Pt (Pt–Au2 = 2.590 (3) Å, P1–Pt–Au2 = 161.5 (5)°) is the shortest, just as in $[(H)(PPh_3)Pt(AuPPh_3)_7]^{2+}$.[4] The Au–Au bond distances in the periphery of **8** (average 2.949 Å, range 2.811 (5)–3.176 (3) Å) are within the range of values, 2.6–3.2 Å,[3,6,10] observed in other Au–Pt clusters containing primarily phosphine ligands. The Pt–P and Au–P bond lengths are normal and within the range observed in other Pt–Au clusters.[2,10] The Au–PPh_3 vectors are approximately trans to the Pt atom (average Pt–Au–P = 167.1°, range 161.1 (6)–172.1 (3)°), which is generally observed in compounds of this type.[2,3,10] The geometry of the CO ligand is normal (Pt–C1 = 1.99 (6) Å, C1–O1 = 1.05 (8) Å, Pt–C1–O1 = 171 (4)°) and identical with that observed in $[(CO)(PPh_3)Pt(AuPPh_3)_6]^{2+}$ (Pt–C = 1.98 Å, C–O = 1.06 Å, Pt–C–O = 175°).[3]

Crystal Structure of $[(PPh_3)Pt(AuPPh_3)_5(HgNO_3)_2](NO_3)\cdot 3CH_2Cl_2$ ($11(NO_3)\cdot 3CH_2Cl_2$). The structure of the coordination core is shown in Figure 2, and selected distances and angles are shown in Table V. The central Pt atom is bonded to give peripheral $AuPPh_3$ units, two peripheral $HgNO_3$ units, and one PPh_3 ligand to give an eight-coordinate platinum atom. The general formulation of **11** including the location of the Pt, Au, and Hg atoms is confirmed by ^{31}P NMR, conductivity, and FABMS data (vide supra), although the fluxionality in the NMR spectrum precluded a determination of geometry. The geometry of the cluster core is best described as a fragment of a Pt-centered icosahedron (vide supra) and is shown in Figure 3. The two Hg atoms lie within the pentagonal plane defined by Au2, Au3, Hg2, Au5, and Hg1 and are separated by Au5 within that plane. The distances (Å) from the weighted least-squares plane for the atoms defining the plane are as follows: Au2, −0.076 (1); Au3, 0.058 (1); Hg2, −0.026 (1); Au5, −0.027 (1); Hg1, 0.086 (1). For the atoms Au1 and Pt, the distances from the plane are −1.65 and 1.00 Å. The Au1 atom symmetrically caps this pentagonal plane and is approximately trans to the PPh_3 bonded to Pt (Au1–Pt–P6 = 164.0 (2)°). This Pt-bound PPh_3 ligand is thus positioned in the direction of the icosahedron vertex labeled A in Figure 3.

The nitrate ligands are bound to the Hg atoms in an unsymmetrical chelated fashion (Hg1–O11 = 2.28 (3), Hg1–O13 = 2.66 (3), Hg2–O21 = 2.32 (3), Hg2–O23 = 2.62 (4) Å). In the case of the nitrate bound to Hg2, the Hg–O bonds are nearly trans to Pt and Au1, respectively (Pt–Hg2–O21 = 177.4 (8), Pt–Hg2–O23 = 172 (1)°), and the Hg–O distance trans to Pt is the shortest. The situation for the nitrate bound to Hg1 is different in that neither Hg–O bond is trans to Pt or Au1 (Pt–Hg1–O11 = 149.8 (7), Pt–Hg–O13 = 156.0 (8), Au1–Hg1–O11 = 155.3 (7), Au1–Hg1–O13 = 104.6 (7)°) and the shorter Hg–O bond is most transoid to Au1. The geometry of the nitrate ligands is otherwise normal. The nitrate counterion was not located in the X-ray analysis, but its presence was confirmed by the IR (KBr) spectrum, which showed the presence of bound (1255 cm^{-1}) and unbound (1341 cm^{-1}) nitrate. Conductivity data also support the monocationic formulation of **11** in solution (vide supra).

The Pt–Hg bond distances in **11** (2.651 (3) and 2.667 (3) Å) are significantly shorter than the 2.928- and 3.045-Å values observed in the only other Pt–Hg–Au cluster, $[Pt(AuPPh_3)_8(Hg)_2]^{4+}$,[8] and Pt_3Hg clusters (average 2.99 Å)[28,29] but are in the wide range of values observed in dinuclear Pt–Hg compounds (2.51–2.83 Å).[30–32] The distances in **11** are longer than the sum of the covalent radii of Pt and Hg (2.532 Å).[32] It is not clear why the Pt–Hg distances in **11** are so much shorter than in $[Pt(AuPPh_3)_8(Hg)_2]^{4+}$; however, the latter complex has much greater steric crowding and its Hg atoms do not have nitrate ligands bound to them.[8] The Au–Hg bond distances (average 2.951 Å, range 2.775 (4)–3.072 (3) Å) are similar to the 3.00-Å average value in $[Pt(AuPPh_3)_8(Hg)_2]^{4+}$.[8] The Pt–Au and Au–Au bond distances (Pt–Au average = 2.680 Å, range 2.647 (3)–2.705 (3) Å; Au–Au average = 2.906 Å, range 2.811 (3)–3.056 (3) Å) are within the range of values observed in other Pt–Au clusters containing primarily phosphine ligands (vide supra) and in $[Pt(AuPPh_3)_8(Hg)_2]^{4+}$ are as follows: Pt–Au average = 2.632 Å and Au–Au range = 2.904–3.38 Å.[8] The Au–P bond lengths (average 2.280 Å) are in the range normally found in gold clusters.[3,6,10]

Summary and Conclusions. A series of Pt-centered $L_yPt(AuPPh_3)_x$ cluster complexes, where x = 2–8, have now been prepared. The Au periphery of these clusters has also been expanded by the addition of one Ag^+ or two Hg^+ metal ions to give $PtAu_8Ag$,[7] $PtAu_5Hg_2$ (**11**, **12**), and $PtAu_8Hg_2$.[8,9] The ligands L bonded to Pt include PPh_3, CO, RC≡C, H, NO_3, CN, halide, $P(OR)_3$, and dppe. In this work we have prepared and characterized the new complexes with x = 3 and 4 (**1**–**6**), several $PtAu_5Hg_2$ clusters (**11**, **12**), and clusters with L = halide (**4**, **5**, **9**), $P(OR)_3$ (**10**), and dppe (**5**, **6**). In addition, we have structurally characterized the x = 5 cluster **8** in the solid state by X-ray diffraction. This study has significantly extended the range and variety of known Pt–Au clusters.

The structures of many of the clusters in this series have been determined in the solid state by X-ray crystallography, and some

(28) Yamamoto, Y.; Yamazaki, H.; Sakurai, T. *J. Am. Chem. Soc.* **1982**, *104*, 2329.
(29) Albinati, A.; Moor, A.; Pregosin, P. S.; Venanzi, L. M. *J. Am. Chem. Soc.* **1982**, *104*, 7672.
(30) Sharp, P. R. *Inorg. Chem.* **1986**, *25*, 4185.
(31) Ploeg, A. F. M. J. v. d.; van Koten, G.; Vrieze, K.; Spek, A. L. *Inorg. Chem.* **1982**, *21*, 2014.
(32) Ghilardi, C. A.; Midollini, S.; Moneti, S.; Orlandini, A.; Scapacci, G.; Dakternieks, D. *J. Chem. Soc., Chem. Commun.* **1989**, 1686.

interesting generalizations can be made. The Pt-centered clusters that have 16 valence electrons have flattened toroidal geometries, while those having 18 electrons have spheroidal geometries usually based on the icosahedron or the cube. This has been explained by the tensor surface harmonics theory introduced by Stone[11,33,34] and extended to include Au clusters by Mingos.[12] Recent work by Kanters et al.[3,6,7,35] and the results reported in this study show that this structural generalization works very well for Pt-centered L_yPtAu_x clusters. For example, the 18-electron clusters shown in Figure 3 all have spheroidal geometries that can be described as icosahedral fragments. In these structures the Pt-bound ligands (PPh_3 or CO) are positioned in the direction of other icosahedral vertices (vide supra). The 18-electron clusters $[(PPh_3)(H)Pt(AuPPh_3)_7]^{2+}$[4] and $[(C{\equiv}C{-}t\text{-Bu})(PPh_3)Pt(AuPPh_3)_6]^{+}$[2] have distorted cubic geometries. The 16-electron Pt-centered clusters $[(PPh_3)Pt(AuPPh_3)_6]^{2+}$,[3] $[Pt(AuPPh_3)_8]^{2+}$,[6] and $[(AgNO_3)Pt(AuPPh_3)_8]^{2+}$[7] all have flattened toroidal geometries. Figures in ref 3, 6, and 7 clearly show the change from toroidal to spheroidal geometry for these three clusters, respectively, upon the addition of the 2-electron-donor ligand CO.

The utility of this simple electron counting formalism in predicting reactivity and structure in clusters of this type has been demonstrated in this and other studies and will guide future work in this area.

Acknowledgment. This work was supported by the National Science Foundation (Grant CHE-8818187) and by the University of Minnesota. We also thank the Fundação De Amparo A Pesquisa Do Estado De São Paulo for support of Dr. Felicissimo's visit to Minnesota. We are grateful for many helpful discussions with Prof. J. J. Steggerda and his co-workers.

Supplementary Material Available: Figures S1 and S2, displaying the PLUTO drawings of **8** and **11**, and Tables SI-SIX, listing complete crystal data and data collection parameters, general temperature factor expressions, final positional and thermal parameters for all atoms including solvate molecules, and distances and angles (30 pages); Tables SX and SXI, listing observed and calculated structure factor amplitudes (86 pages). Ordering information is given on any current masthead page.

(33) Stone, A. J. *Mol. Phys.* **1980**, *41*, 1339.
(34) Stone, A. J. *Polyhedron* **1984**, *3*, 1299.
(35) Kanters, R. P. F. Ph.D. Thesis, Nijmegen, The Netherlands, 1990, ISBN 90-9003290-8.

Contribution from the Department of Chemistry, University of Victoria, Victoria, British Columbia, Canada V8W 3P6

Synthesis and ^{31}P NMR Spectroscopy of Trinuclear, Phosphido-Bridged Iridium and Rhodium Clusters. Crystal and Molecular Structures of $[M_3(\mu\text{-}PPh_2)_3(CO)_nL_2]$ (M = Ir or Rh, n = 3, L_2 = Bis(diphenylphosphino)methane; M = Ir, n = 5, L = *t*-BuNC)

David E. Berry, Jane Browning, Khashayar Dehghan, Keith R. Dixon,* Neil J. Meanwell, and Andrew J. Phillips

Received June 14, 1990

Reaction of $[Ir_2(cyclooctene)_4Cl_2]$ with CO, $NHEt_2$, and $PHPh_2$ provides a synthetic route to the trinuclear, phosphido-bridged iridium clusters $[Ir_3(\mu\text{-}PPh_2)_3(CO)_nL_2]$ (n = 3, L = CO or PPh_3, L_2 = bis(diphenylphosphino)methane (dppm); n = 5, L = *t*-BuNC). The CO and PPh_3 complexes are analogues of previously known rhodium derivatives, and rhodium analogues of the dppm and *t*-BuNC complexes are also reported. $[Ir_3(\mu\text{-}PPh_2)_3(CO)_3(dppm)]$ (I) and $[Rh_3(\mu\text{-}PPh_2)_3(CO)_3(dppm)]$ (II) crystallize in the *Pnma* space group (Z = 4) with the following respective unit cell dimensions: a = 23.963 (5) Å, b = 24.970 (5) Å, c = 11.080 (2) Å; a = 24.031 (6) Å, b = 25.069 (9) Å, c = 11.117 (4) Å. $[Ir_3(\mu\text{-}PPh_2)_3(CO)_5(t\text{-BuNC})_2]$ (III) crystallizes in the $P2_1/n$ space group (Z = 4) with a = 23.015 (4) Å, b = 20.197 (6) Å, c = 11.849 (5) Å, and β = 92.19 (4)°. The structures of I and II consist of approximately equailateral triangles of metal atoms (average M-M distances 2.78 (Ir) and 2.79 Å (Rh)), with the CO and two PPh_2 ligands lying approximately in the M_3 plane. The third PPh_2 bridge is approximately perpendicular to this plane, linking the two basal metal atoms, which are also bridged by the dppm ligand. In contrast, the structure of III has all three PPh_2 bridges approximately in the M_3 plane with the *t*-BuNC ligands added approximately perpendicular to this plane at the apical iridium. The Ir-Ir distances are much longer, averaging 3.23 Å. Complete analyses of ^{31}P NMR spectra are reported for I-III and for IV, the Rh analogue of III. The phosphido bridge shifts reflect the changes in metal-metal distances, with I and II strongly deshielded (by 80-240 ppm) relative to III and IV. There is also a general reduction in the one-bond Rh-P coupling constants in the 50-electron cluster, IV relative to the 46-electron cluster, II.

Introduction

A recurring theme of recent organometallic and cluster chemistry has been the study of metals linked by strong yet flexible bridges. Such bridges are able to preserve the integrity of a complex while permitting the making and breaking of metal-metal bonds. Two notable examples are the extensive studies of "A-frame" complexes in which two metals are linked by bis(diphenylphosphino)methane (dppm) bridges[1,2] and also the interest in phosphido (PR_2) bridges in both dinuclear and cluster complexes.[3-10] The trinuclear cluster $[Rh_3(\mu\text{-}PPh_2)_3(CO)_5]$[11,12] is an especially interesting example of the latter, involving one formal 16-electron metal center and two 18-electron centers. There are 46 cluster valence electrons, and the Rh-Rh bonds average 2.77 Å. In a carbon monoxide atmosphere, this complex can be converted to an unstable 50-electron derivative, $[Rh_3(\mu\text{-}PPh_2)_3(CO)_7]$, in which there are formally two 16-electron centers and one 18-electron center and in which the Rh-Rh distances average 3.15

(1) Puddephatt, R. J. *Chem. Soc. Rev.* **1983**, *12*, 99-127.
(2) Balch, A. L. In *Catalytic Aspects of Metal Phosphine Complexes*; Alyea, E. C., Meek, D. W., Eds.; Advances in Chemistry Series 196; American Chemical Society: Washington, DC, 1982; pp 243-255.
(3) Carty, A. J. In ref 2, pp 163-193.
(4) Yu, Y. F.; Chau, C. N.; Wojcicki, A.; Calligaris, M.; Nardin, G.; Balducci, G. *J. Am. Chem. Soc.* **1984**, *106*, 3704-3705.
(5) Regragui, R.; Dixneuf, P. H.; Taylor, N. J.; Carty, A. J. *Organometallics* **1984**, *3*, 1020-1025.
(6) Patel, V. D.; Taylor, N. J.; Carty, A. J. *J. Chem. Soc., Chem. Commun.* **1984**, 99-100.
(7) Regragui, R.; Dixneuf, P. H.; Taylor, N. J.; Carty, A. J. *Organometallics* **1984**, *3*, 814-816.
(8) Geoffroy, G. L.; Rosenberg, S.; Shulman, P. M.; Whittle, R. R. *J. Am. Chem. Soc.* **1984**, *106*, 1519-1521.
(9) Shyu, S. G.; Wojcicki, A. *Organometallics* **1984**, *3*, 809-812.
(10) Carty, A. J.; Maclaughlin, S. A.; Nucciarone, D. In *Phosphorus-31 NMR Spectroscopy in Stereochemical Analysis*; Verkade, J. G., Quin, L. D., Eds.; VCH Publishers Inc.: New York, 1987; pp 559-620.
(11) Haines, R. J.; Steen, N. D. C. T.; English, R. B. *J. Organomet. Chem.* **1981**, *209*, C34-36.
(12) Haines, R. J.; Steen, N. D. C. T.; English, R. B. *J. Chem. Soc., Dalton Trans.* **1984**, 515-525.

0020-1669/91/1330-0396$02.50/0